

Sensitivity analysis of wind turbine fatigue reliability in wind turbines: effects of design turbulence and the Wöhler exponent

Shadan Mozafari^{1,*}, Paul Veers², Jennifer Marie Rinker¹, and Katherine Dykes¹

¹Department of Wind Energy, Technical University of Denmark, Roskilde, Denmark

²National Renewable Energy Laboratory (NREL), Golden, CO, USA.

Correspondence: Shadan Mozafari (Shad.mzf@gmail.com)

Abstract.

Fatigue reliability assessment of wind turbines involves three major sources of uncertainty: material resistance, loads, and the damage accumulation model. Many studies focus on increasing the accuracy of fatigue load assessment for improving the fatigue reliability. Probabilistic modeling of the wind's decreasing the uncertainty in fatigue load assessments via different approaches including more detailed characterization of the turbulence standard deviation is an example approach for this purpose.

Editions (turbulence) in the design phase. The IEC standard suggests two different distributions in Edition 3 and Edition 4 of the IEC standard for the design of wind energy generation systems (IEC 61400-1) suggest different probability distributions as alternatives for the representative turbulence in the normal turbulence model its Normal Turbulence Model (NTM) of Edition 4: lognormal and Weibull. There are debates on whether the two suggested distributions provide conservative reliability levels, as adequately safe reliability in relevant load channels since the established design safety factors are calibrated based on the representative turbulence approach. The current study addresses the debate by comparing annual reliability based on different scenarios of NTM using a probabilistic approach. More importantly, it elaborates on the relative importance of load assessment accuracy in defining the fatigue reliability level of importance of this matter or most of the other concerns about the load's uncertainty in the context of reliability considering all uncertainty in the material properties and the linear damage accumulation rule.

Using the DTU 10-MW aeroelastic simulations of the DTU 10MW reference wind turbine and the first-order reliability method (FORM) a simple model for assessing fatigue reliability based on the distribution of damage equivalent load (DEL), we study the changes and the trends in the annual reliability level and its sensitivity to the three main random inputs. We perform the study considering the as well as the relative importance of each of the uncertainty groups. In addition, we investigate the effects of different fatigue exponents on the overall results in the blade root flapwise and the tower base fore-aft moments assuming different fatigue exponents in each load channel load channels.

The results show that integration over distributions generally using the distribution of turbulence in each mean wind speed results in less conservative annual reliability levels than compared to representative turbulence. The difference in the reliability levels varies according to turbulence distribution and the fatigue exponent. In the case of the tower base, the difference in the annual reliability index reliability after 20 years can be up to 50%50%. However, the model and material uncertainty have much

higher effects on the reliability levels compared to ~~load-DEL~~ uncertainty. Knowledge about such differences in the reliability levels due to the choice of turbulence ~~distribution characterization method~~ is especially important, as it impacts the extent of lifetime extension through reliability ~~reassessments~~ re-assessments.

30 **keywords:** Wind turbine reliability, Fatigue reliability, Uncertainty quantification, Sensitivity analysis, Normal Turbulence Model, Turbulence distribution

1 Introduction

~~Fatigue~~ The fatigue reliability of a structure is its ability to withstand cyclic loading during the design ~~life~~ lifetime. Fatigue life is a highly sensitive and uncertain variable (Veers, 1996). In the case of wind turbines, the random and variable amplitude loading and the complexity of the structural system increase such uncertainty. In addition, there is a high level of uncertainty in material strength ~~and in data and~~ the simplified models commonly used for counting cycles or describing the material properties and damage accumulation. The probabilistic approach for fatigue reliability assessment involves probabilistic modeling of the crucial random inputs leading to a more robust analysis and design of the wind turbines against fatigue (Choi et al., 2007). The IEC design standard introduces a semi-deterministic approach that includes safety factors to account for the uncertainty in different inputs. These factors are calibrated based on probabilistic reliability assessment aiming at an acceptable target reliability level at the end of ~~design life~~ Treatment of the uncertainty of the different random inputs operation time (design lifetime). It is clear that the uncertainty analysis of the mentioned sources is an important part of the probabilistic reliability assessment. Fig. 1 shows the general schematic view of the main random inputs of the fatigue reliability assessment considered in the current study.

45 Stensgaard et al. (2016a) show that wind climate parameters contribute to about 10%–30% of the total uncertainty in the reliability estimation. Furthermore, the sensitivity analysis results in (Stensgaard et al., 2016a; Dimitrov et al., 2018; Robertson et al., 2019; Murcia et al., 2018) reveal that after the mean wind speed, the standard deviation of the wind (turbulence) has the largest impact on the equivalent fatigue load levels in most of the load channels. Thus, accurate modeling of the turbulence at 50 the design level is crucial for decreasing the uncertainties in the fatigue loads.

The IEC standard (IEC 61400-1, 2005) suggests the Normal ~~Turbulence Model (NTM)~~ turbulence model. The model is mainly based on a representative value in each wind speed bin for estimating turbulence. The representative value is the 90% quantile of a lognormal distribution. However, the standard also ~~allows~~ keeps the option of using the whole ~~lognormal~~ distribution instead of a single value distribution open for the designer. Edition 4 of the IEC standard (IEC 61400-1, 2019) suggests a Weibull distribution with the same 90% quantile magnitude.

~~Some studies investigate~~ There are some studies investigating the performance of ~~different NTM approaches~~ the different approaches of NTM in describing the site turbulence conditions. For example, Ren et al. (2018) investigated the ~~suitability~~

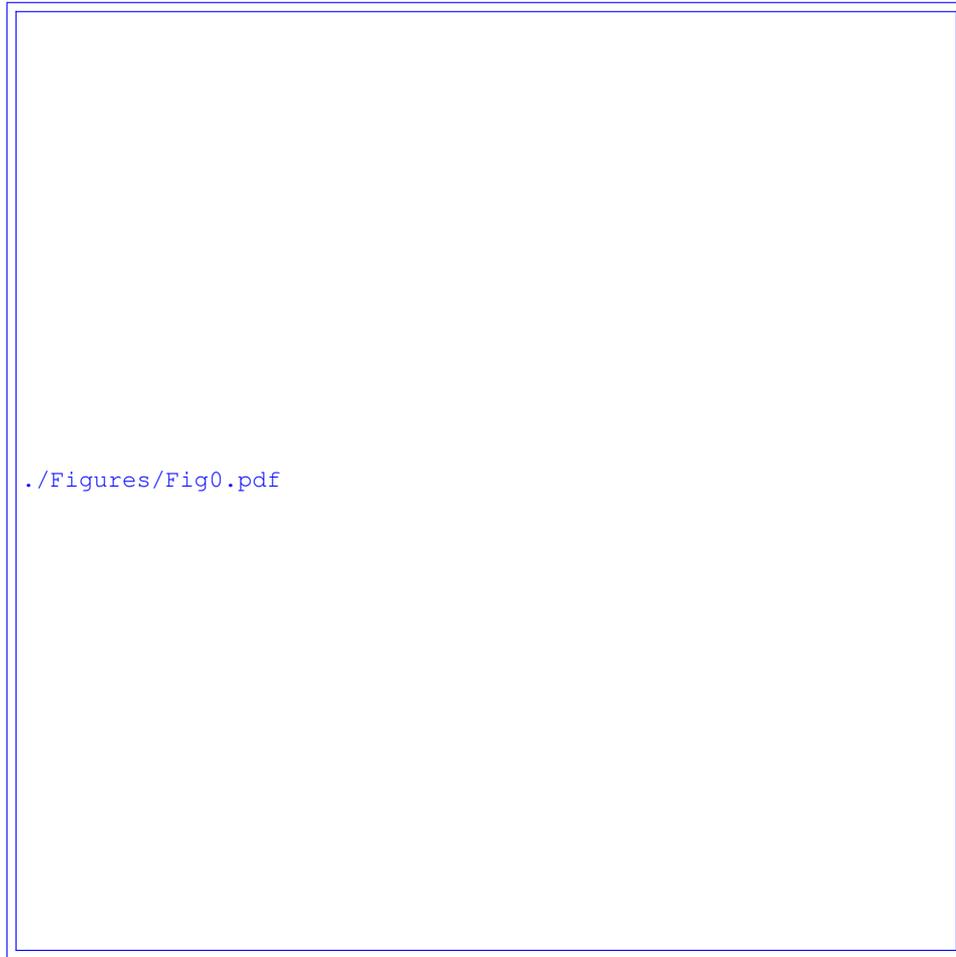


Figure 1. Flowchart of the main random inputs (X_i) and the output (Y) in the fatigue reliability assessment

60 ~~of the compatibility of~~ 90% quantile recommendation for describing onshore conditions and showed that it overestimates the turbulence. Thus, they proposed a three-parameter power-law model for turbulence intensity. In addition, Øistad (2015) investigated the performance of representative turbulence recommendations on a case with both onshore and offshore wind conditions and concluded that the model overestimates the turbulence levels in both cases. ~~Other similar studies focused~~ There are more similar studies focusing on offshore conditions (Wang et al., 2014; Türk and Emeis, 2010; Tsugawa et al., 2015) ~~show~~ showing the inaccuracy of the IEC standard recommendations ~~in representing the turbulence in compared to~~ real wind fields. In addition, Ishihara (2012) ~~presented~~ presents the same results by studying the compliance of the lognormal distribution of the IEC standard with measurements in an offshore wind farm. As another example, Dimitrov et al. (2017) ~~showed that for a show that for their~~ case study site, the lognormal distribution provides ~~overconservative turbulence expectations, over-conservative turbulence expectations~~ and thus, ~~it suggests a suggests~~ 2-parameter Weibull distribution. ~~Emies (2014) showed~~ The results of (Søndergaard and Jóhannsson, 2016) also conclude lognormal to be conservative. They suggested Weibull distribution as a

65

70

better (less conservative choice) in the case of blade fatigue and extreme loads. Emies (2014) shows an offshore case within which the IEC Normal ~~Turbulence Model provides underconservative~~ turbulence model provides under-conservative results for turbulence intensity in low mean wind speeds and over-conservative values in higher mean wind speeds. A few studies like (Larsen, 2001; Wang et al., 2014) explicitly ~~introduceed~~ introduce other approaches for modeling offshore turbulence ;
75 ~~as they proposed that the NTM is overconservative~~ as they propose that the Normal turbulence model of the IEC standard is over-conservative for all offshore cases.

In addition, there are some studies on the loads corresponding to each turbulence characterization approach. The results of these studies vary from each other. For example, some pieces of research like (Ernst et al., 2012; Dimitrov et al., 2017; Hansen
80 and Larsen, 2005) ~~showed~~ show that the IEC representative and ~~full lognormal distribution models of turbulence~~ lognormal turbulence models are very conservative in the case of blade loads and ~~proposed~~ propose new, less conservative turbulence models. ~~The results of Søndergaard and Jóhannsson (2016) also conclude that the lognormal assumption is conservative. They suggested the Weibull distribution as a less conservative choice in terms of resulting blade fatigue and extreme loads.~~ On the other hand, the results of (Stensgaard et al., 2016a) show that following the ~~suggested~~ suggestion on 90% quantile level for
85 turbulence in the IEC standard leads to an accurate assessment of the blade root flapwise bending moment while producing a conservative assessment of the tower bottom fore-aft bending moment and low-speed shaft torque. It has to be noted that these comparisons are ~~made done~~ with real data in which the wind shear is also variable (and a function of turbulence) ; ~~and affects the~~ and it can greatly affect special load channels.

90 As a second matter, the effect of uncertainty in the material properties on fatigue reliability assessment is also covered in many studies. According to previous research, like (Veers, 1996; Zaccone, 2001), the uncertainty inherent in the material properties ; including physical, modeling, and measurement uncertainty ; ~~represents~~ represent almost half the total uncertainty ~~in the fatigue damage~~. The results of the sensitivity analysis in (Velarde et al., 2020)) and ~~Ronold et al. (1999) showed~~ (Ronold et al., 1999) show that the uncertainties related to the material resistance model have the ~~greatest~~ highest influence on
95 fatigue reliability. Bacharoudis et al. (2015) presented the high sensitivity of wind turbine blade reliability to the measurement uncertainty in the material properties of the composites using the DTU 10-MW wind turbine as the case study.

All in all, there are many studies on the level of accuracy and performance of the representative turbulence ; ~~suggestion~~ and they all show the need for transition from such a model to lognormal and Weibull distributions ; especially in the case of
100 offshore wind farms with ~~overall~~ lower turbulence levels. However, they have not compared different scenarios to each other in general design conditions ; ~~It is still debated whether~~ and it is still under debate if the two distributions always provide ~~lower safe~~ safe reliability levels for different load channels ~~compared to the representative value approach~~. The current work addresses this gap and such debate. Knowing the difference between the reliability levels when following different NTM approaches is especially important because the established safety factors for the semi-deterministic approach in the IEC design standard
105 are calibrated based on the representative turbulence approach. Thus, ~~if reliability levels are assessed~~ one should be aware

that if they assess the reliability levels using the same safety factors while characterizing the standard deviation turbulence by distribution, the semi-deterministic approach and probabilistic approach do not meet at the same reliability level at the end of the design life component's design lifetime. It is important to ensure make sure that the two alternative distributions are never underconservative under-conservative. Furthermore, knowing the differences in reliability levels having information about the level of differences can be an asset for fast initial estimation of the possible extension of a lifetime when only by knowledge about the considered approach in the design phase is known. Such. It is clear that such information about the design assumptions is also crucial for more accurate lifetime extension assessments in the more detailed assessments of lifetime extension using site-specific data.

115 In addition, considering the results of the previous studies on the importance of material uncertainty in fatigue reliability, it is valuable to investigate study how all the efforts for accurate modeling characterization of the turbulence will transfer to a more robust reliability assessment accurate reliability assessment considering the high uncertainty in material properties and model. In the present study, we reveal how different approaches in the IEC standard for a general case can change the distribution of the fatigue loads. We also In addition, we study the sensitivity of the reliability to the change in the fatigue load compared to its sensitivity to variations in other random inputs.

The results of the current study cover blade flapwise and tower base fore-aft load channels in a large wind turbine (10-MW) from IEC class 1A. We study the difference differences in distributions of the damage equivalent load (DEL) considering different NTM representations using many DEL in different suggestions of the IEC standard regarding turbulence using a large number of aeroelastic simulations and bootstrapping technique. In addition, the results show the overall relative importance of DEL variation due to turbulence model by revealing the relative effects of load uncertainty on the reliability. Knowing the extent to which the various sources of uncertainty affect reliability can help by comparing its effect with two other major sources of uncertainty in the fatigue reliability assessment. The knowledge about the importance factors is a guide for designers and researchers focus on effective areas to get showing where they should put their focus and efforts regarding reducing uncertainty to get more robust reliability levels. The fatigue exponent is the exponent to which the load is powered in the damage models commonly used (as in the current study). Thus, it directly changes the share of the loads in the fatigue damage, and it. This parameter also changes the distribution of DEL (Mozafari et al., 2023). We, thus, we also investigate the results of the reliability study in different fatigue exponent levels in each load channel. An important note is that since the DTU 10-MW turbine is not designed against fatigue, we observed low reliability low-reliability levels in the blade root and the tower base. Thus, and thus the mean value of the material properties is scaled while keeping the coefficient of variation the same. To lower the errors in the first-order reliability method (FORM) in the case of the blade (high fatigue exponent and thus high nonlinearity), we calibrate the mean material strength to obtain lower probabilities of failure for the sake of accuracy. The are scaled and the reliability levels are therefore not based on real data. In other words, the trends and effects, which are the purpose of the current study, are reliable, are reliable but the reliability levels are not.

140

~~We~~ In the following sections, first, we provide information about the wind turbine case study ~~and in Sect. 2.1 and the characteristics of the~~ the aeroelastic simulations in ~~in Sect. 2.1 and Sect. 2.2, respectively.~~ Sect. 2.3-2.2. In addition, Sect. 3.1 provides information about the assumptions and the mathematical relations used in the current study for assessing fatigue loads, post-processing simulation results ~~-, reliability assessment-, as well as reliability assessment~~ and sensitivity analysis methods. 145 Then, Sect. 3 presents the results in three parts: Sect. 3.1 covers the results of DEL distributions, Sect. 3.2 shows the results of the reliability assessments ~~-, and~~ Sect. 3.3 provides the sensitivity analysis of the reliability. Finally, Sect. 4 contains the conclusions of the study ~~together with limitations,~~ limitations, and suggestions for future research in the area.

2 Methodology

We use 10-minute aeroelastic simulations to obtain the load time series and estimate the fatigue reliability based on them. Fig. 1 ~~presents a general, schematic view of the main random inputs of the fatigue reliability assessment and the procedure for the analysis in the current study. The following sections will provide more details.~~ 150

~~Flowchart of the procedure, main random inputs (X_i), and the output (Y) considered in the present study for the fatigue reliability assessment~~

Sect. 2.1 explains the specifications of the case study wind turbine ~~specifications,~~ and Sect. 2.2 introduces the properties of 155 the simulations. Finally, ~~Sect. 2.3~~ explains the mathematical relations and methods we use.

2.1 The case study wind turbine

~~Our case study is the DTU 10-MW~~ We consider the DTU 10MW reference wind turbine (Bak et al., 2013) as our case study. The DTU ~~10-MW is 10MW is an offshore wind turbine~~ from IEC standard class 1A (IEC 61400-1, 2019) with a rotor diameter of 178.3 ~~m-meters~~ and a hub height of 119 ~~mmeters~~. It is rated at a power of 10 MW and a mean wind speed of 11.4 m/s. 160 The cut-in and cut-out mean wind speeds are 4 m/s and 26 m/s, respectively. The blade in the current case study is made of unidirectional E-glass fiber epoxy ~~-, and~~ the tower is made of steel. ~~In the present study, we use the onshore version of the DTU 10-MW wind turbine.~~

2.2 Aeroelastic simulations

We perform three groups of ~~aeroelastic simulations in HAWC2¹ software (Larsen and Hansen, 2007),~~ simulations, representing 165 three case studies, forming a total of ~~98,400~~ 98400 10-minute aeroelastic simulations of the DTU 10-MW reference wind turbine ~~-. Each simulation group covers an approach for modeling in HAWC2¹ software (Larsen and Hansen, 2007). The difference between the three groups lies in the modeling of~~ turbulence (standard deviation of wind) in wind speed bins. ~~The current work only covers normal operating conditions and does not consider~~ different wind speed levels. Although fatigue can occur in different conditions, in the current work, we only consider operational conditions and not the fatigue damage ~~occurring~~

¹ ~~An aeroelastic code for calculating wind turbine response in the time domain—developed in DTU Wind energy department between years 2003-2007~~

¹ An aeroelastic code for calculating wind turbine response in the time domain- developed in DTU Wind energy department between years 2003-2007

170 ~~in the fault, idling, due to the~~ start-up or shutdown events ~~for simplicity~~. Thus, we perform the simulations based on IEC standard ~~design load case (DLC) DLC 1.2 (IEC 61400-1, 2019) with normal wind condition~~ load case (IEC 61400-1, 2019) with Normal wind conditions. As another simplification, we set the wind direction constant ~~and~~ equal to zero in all the simulations. The mean wind speed (MWS) varies from 4 m/s (cut-in) to 26 m/s (cut-out) in bins of size 2 m/s. ~~Simulations are performed for 700 s, from which the first 100 s is recognized as transient time and are omitted from the results. The transient time is~~
175 ~~defined by checking the time of stabilization for tower base side-side moments in high mean wind speeds (20–26 m/s), as this load channel is the one with the longest stabilization time.~~ We use the Mann turbulence model ~~for modeling, which is a method for simulation of~~ the wind field (see (Mann, 1998)). ~~The Mann turbulence boxes contain 8,192, for generating the turbulence boxes in the simulations. The boxes contain 8192~~ evaluation points in the wind direction for higher resolution and 32 points in ~~each of~~ the other two perpendicular directions. Each wind bin (a combination of wind speed and turbulence) ~~has consists of~~
180 200 turbulence realizations. ~~We use 200 turbulence seeds, as the results of a previous study (Mozafari et al., 2023) show that the estimation of the fatigue loads fairly converges in this number of realizations.~~ Table 1 presents the specifications of wind load modeling in each group of simulations.

Table 1. Specifications of wind modeling in three groups of HAWC2 simulations corresponding to three study cases

| Parameter | Group 1 | Group 2 | Group 3 |
|--|----------|--|---------|
| Marginal distribution of turbulence | constant | lognormal <u>Log-normal</u> | Weibull |
| Turbulence levels in each mean wind speed <u>MWS</u> bin | 1 | 20 | 20 |
| Realizations per wind condition | 200 | | |
| Wind shear exponent | 0.2 | | |
| Turbulence model | Mann | | |
| Cut-in mean wind speed (m/s) <u>(m/s)</u> | 4 | | |
| Cut-out mean wind speed (m/s) <u>(m/s)</u> | 26 | | |
| Rated wind speed (m/s) <u>(m/s)</u> | 11.4 | | |
| Size of wind speed bins (m/s) <u>(m/s)</u> | 2 | | |
| Mean wind speed distribution | Rayleigh | | |
| Yaw angle (degrees) | 0 | | |
| Simulation time (seconds) Initial transient time (seconds) Mann box grids along the wind | 8192 | | |
| Mann box grids in other dimensions | 32 | | |
| Time steps of the simulations (ssec) <u>(ssec)</u> | 0.01 | | |

~~The study considers~~ We consider the flapwise bending moment in the blade and the fore-aft bending moment in the tower base as the main outputs of the simulations and the input for the fatigue assessment of the blade and tower base.

185 2.3 Mathematical formulations

In the following, we present the mathematical background and relations ~~we use for post-processing that we use to post-process~~ simulation load outputs and ~~estimating estimate~~ the corresponding fatigue damage and reliability.

2.3.1 Probabilistic modeling of wind

The wind as a random process is mostly described by its mean value and standard deviation (turbulence) at each point of time
190 and space. The IEC standard (IEC 61400-1, 2019) presents a Rayleigh distribution for probabilistic modeling of the mean wind
speed at the wind turbine's hub height. ~~Equation Eq.~~ (1) presents the cumulative distribution function (CDF) of the mean wind
speed based on the suggested Rayleigh distribution.

$$F(V_{hub}) = \frac{1 - e^{-\pi(\frac{V_{hub}}{2V_{ave}})^2}}{1 - \exp(-\pi(\frac{V_{hub}}{2V_{ave}})^2)} \quad (1)$$

In Eq. (1), $F(V_{hub})$ is the CDF. Furthermore, V_{hub} accounts for the mean wind speed at the hub height, ~~and V_{ave} and~~
195 v_{ave} is the annual mean wind speed at the hub height. In the standard wind turbine classes, ~~$V_{ave} = 0.2V_{ref}$ $v_{ave} = 0.2v_{ref}$~~ in
which the ~~V_{ref} v_{ref}~~ is the 50-year extreme wind speed over 10 minutes. The parameter ~~V_{ref} equals v_{ref} is equal to~~ 50 m/s in
the IEC class 1 category (IEC 61400-1, 2019), ~~which is~~ the class of the current case study wind turbine.

The statistical parameters of the wind are correlated. In other words, the standard deviation of the wind (~~turbulence~~) changes
with a change in the mean level. However, since the IEC design standard suggests binning of the wind speeds (as we do in our
200 simulations), one can use the marginal distribution of turbulence in each wind speed bin. The ~~third edition of the IEC standard~~
(IEC 61400-1, 2005) presents a lognormal distribution as the marginal distribution of turbulence within each wind speed level.
The fourth edition (IEC 61400-1, 2019) suggests Weibull distribution. Following each of the distributions, the designer is
provided with two options in the IEC standards. The first option is to consider the constant representative turbulence for each
wind speed bin, equal to 90% quantile of the distribution, instead of the marginal distribution. The other option is to consider
205 the whole distribution domain in each wind speed bin. ~~The third edition of the IEC standard (IEC 61400-1, 2005) presents a~~
~~lognormal distribution as the marginal distribution of turbulence (standard deviation of the wind speed) within each wind speed~~
~~level. The fourth edition (IEC 61400-1, 2019) suggests the Weibull distribution. Following each distribution, the designer has~~
~~two options in the IEC standards.~~

The current study investigates the impact of NTM turbulence characterization choice on design fatigue reliability, ~~as it has~~
210 not been studied before. For this purpose, we define three cases for the different turbulence characterization approaches: case
1 covers the 90% quantile turbulence value, and cases 2 and 3 refer to the lognormal and Weibull distributions, respectively.
~~Equations (??), (2), and Equation (2) and Eq.~~ (3) show the ~~CDF, standard deviation, standard deviation~~ and mean of ~~turbulence~~
of the suggested lognormal distribution ($T \sim LN(\mu_T, \sigma_T)$), respectively (case 2). In addition, Eq. (4) shows the 90% quantile
value of the same distribution (case 1).

$$215 \quad F(T) = 0.5 \left(1 + \operatorname{erf} \left(\frac{\ln(T) - \mu_T}{\sigma_T \sqrt{2}} \right) \right) \quad \sigma_T = \sqrt{\ln \left(\left(\frac{I_{ref}(1.4(\text{m/s}))}{0.75V_{hub} + 3.8(\text{m/s})} \right)^2 + 1 \right)} \sqrt{\ln \left(\frac{(I_{ref})^2}{0.75V_{hub} + 3.8} + 1 \right)} \quad (2)$$

$$\mu_T = \ln \left(\frac{I_{ref}(0.75V_{hub} + 3.8)}{I_{ref}} \right) - \frac{(\sigma_T)^2}{2} \quad (3)$$

$$\underline{T_{rep.} = I_{ref}(0.75V_{hub} + 5.6(\text{m/s}))}$$

$$\underline{T_{rep.} = I_{ref}(0.75v_{hub} + 5.6)} \quad (4)$$

220 Equations In Eq. (2) and (3) refer to the NTM model in (IEC 61400-1, 2005). In these equations, T represents turbulence standard deviation, and to Eq. (4), I_{ref} is the reference turbulence intensity equal to 0.16 for the standard class 1 wind turbines (the current case study). In addition, μ_T and σ_T are the mean and standard deviation of the turbulence as a function of the hub height wind speed (V_{hub}) and $T_{rep.}$ is the representative turbulence equal to 90% quantile of the lognormal distribution. One must note that Eq. (4) is not the exact calculation of the representative turbulence and is only a linear regression approximating it.

225 Equations (??), (5), and Equation (5) and Eq. (6) present the CDF (considering that the turbulence always has positive values), the shape parameter, and the shape and scale parameters of the Weibull distribution ($T \sim Wbl(K, C)$), which the fourth edition of the IEC standard (IEC 61400-1, 2019) suggests.

$$\underline{Fk = I_{ref}(T0.27v_{hub} + 1.4) = 1 - e^{-\left(\frac{T}{C}\right)^K}} \quad (5)$$

$$230 \quad \underline{KC = 0.27V_{hub} + 1.4(3.3)} \quad (6)$$

$$\underline{C = I_{ref}(0.75V_{hub} + 3.3(\text{m/s}))}$$

In Eqs In Eq. (5) and (6), K and C represent the shape and scale parameters of the Weibull distribution, respectively. Weibull is very flexible a very flexible distribution and can be close to many other distributions, including lognormal, including lognormal depending on its shape parameter. Figure Fig. 2 presents the cumulative probability distributions of cases 2 and 3 in one mean wind speed of 8 m/s. In this plot, the horizontal axis shows turbulence (T) levels and vertical axis refers to

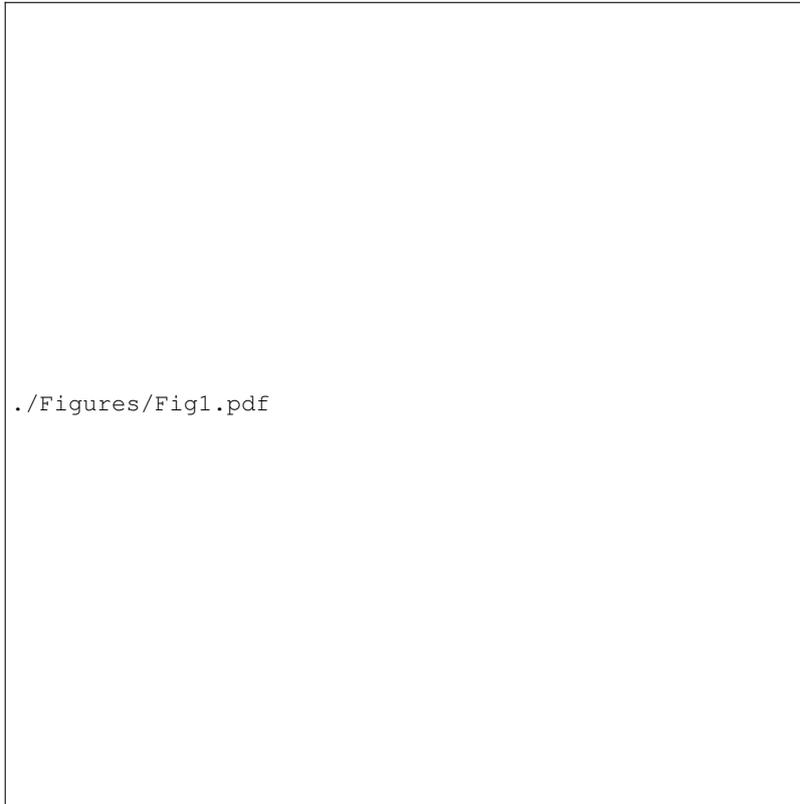


Figure 2. Lognormal and Weibull distribution of turbulence at mean wind speed (MWS) of 8 m/s compared to the 90% quantile level (representative turbulence level)

$\log_{10}(1 - F(T))$, where $T \sim LN(\mu_T, \sigma_T)$ and $T \sim Wbl(K, C)$.

The lognormal distribution is generally heavy-tailed ;however, and as Fig. 2 shows ,for the distribution parameters provided in the standard, NTM with Weibull distribution it has a thicker tail compared to the Weibull distribution in the example. In other words, with the same accumulated probability in the tail (for example ,the 10% upper tail), the Weibull-lognormal tail covers lower turbulence levels than the lognormal distribution and shows higher standard deviation. Overall Weibull distribution. The thin tail of the Weibull distribution and relatively lower mean value (as seen in Fig. 2) also leads to high standard deviations. All in all, the two distributions have opposite behaviors in the two portions before and after their intersection at 90% quantile. The Weibull distribution represents higher probabilities in the lower turbulence levels and covers more data from lower values considering the same number of observations. Therefore, we generally expect the use of the Weibull distribution to represent turbulence occurrences in general, we expect using the Weibull distribution for representing the occurrences of turbulence to be a less conservative approach. In the following sections, we We study this expectation and its effects on the DEL estimations in each case in the following sections.

2.4 Resistance and damage models

250 Material fatigue resistance tests are often performed under constant-amplitude cyclic loading. The information regards the number of cycles that the in each stress amplitude level that a test specimen can endure in each stress amplitude before failing is collected within S-N curves. Basquin formulation (Basquin, 1910) is a linear regression of the $\log N - \log S$ data points valid for most materials in the region between approximately 10^3 and 10^6 cycles. Equation (7) $1e3$ and $1e6$ cycles, where a linear fatigue behavior of the material in a log-log plot is expected. Equation 7 shows the Basquin relationship.

$$255 \quad N = kS^{-m} \quad (7)$$

In Eq. (7), N is the number of endured (allowed) cycles in the stress amplitude equal to S . Both m (the fatigue exponent, also known as Wöhler's exponent) and k (the Basquin coefficient) in Eq. (7) are material-specific. The Basquin regression model is uncertain. In addition, there is also physical and measurement uncertainty included in the material properties and the fatigue tests. In the Basquin representation, m and k reflect the same sources of uncertainty because as they are strongly correlated (an increase of one decreases the other in the regression). Thus, it is enough to model only one of them as the random variable to describe the scatter of the fatigue strength test data (Kececioglu, 2002; Veers, 1996). Following the mentioned common approach, we only consider the variability in the k parameter in the $\log N - \log S$ curve and assume Wöhler's exponent to be deterministic. Considering available data regarding Following available data regards average values of m , we assume the constant fatigue exponent to be equal to 10 in the composite case and equal to 3 in the case of steel components. Thus, we consider two values since we study the blade's flapwise and the tower base fore-aft load channels, we consider two different cases of $m = 10$ and $m = 3$ corresponding to the blade and the tower, respectively. We consider the both compression-compression fatigue data (load ratio of $R = 10$) and tension-tension fatigue data for the fatigue analysis of the flapwise in the case of the flapwise bending moments according to Mikkelsen (2020) (Mikkelsen, 2020) and the resulting time series of the current study.

270 For variable loading, as in the case of In the case of variable loadings, such as in wind turbines, one should use a suitable model to relate the constant amplitude data to the accumulated damage. Palmgren–Miner (Miner's) rule (Palmgren, 1924; Miner, 1945) is a common linear model for this purpose. Equation (8) with the same application. Equation 8 presents Miner's rule.

$$275 \quad D = \sum_{i=1}^{N_s} \frac{n_i}{N_i} \quad (8)$$

In Eq. (8), parameter D accounts for the magnitude of fatigue damage, n_i is the number of cycles of the i th load amplitude in the loading, and N_i is the allowed number of cycles according to the S-N curve of the material. In addition, N_s accounts for the total number of stress amplitude levels. According to the Miner's rule, failure happens when the summation in Eq. (8) is higher than the material limit, often assumed equal to unity.

280 The blade's root ~~cross-section~~ cross-section in the case study wind turbine is nearly circular ~~, and we assume it to be~~ circular in the current study ~~assumes the same. In addition, the pitch angle in the blade root is zero. Thus, the moments along~~ the x and y axes refer to flapwise and edgewise moments, respectively. In both cross-sections. In both cross-sections of the blade root and the tower base, Eq. (9) can represent the relation between the moments and stresses.

$$S_i = \frac{Mx_i c}{I_y} \frac{Mx_i c}{I_y} \quad (9)$$

285 In Eq. (9), Mx_i is the moment corresponding to the stress level S_i . In the ~~present-current~~ present-current study, the direction y corresponds to the global direction of the wind in the HAWC2 simulations since we are considering the root in the blade, and the local coordinate system of the tower base section is also aligned with the global coordinate system. Thus, we consider moments in the perpendicular direction (Mx). In addition, the section parameters c and I_y are the radius and the moment of inertia in the direction ~~of the wind (perpendicular to Mx)~~ perpendicular to the moment's direction, respectively. Table 2 presents the values
290 for c and I_y parameters in the blade's root and tower base ~~cross-sections~~ cross-sections in the structural model of ~~the DTU~~ 10-MW-DTU 10MW reference wind turbine.

Table 2. Blade root and tower base section parameters of the DTU ~~10-MW-10MW~~ 10-MW-10MW model in HAWC2

| Cross section | radius <u>radius</u> (m) | In-plane moment of inertia (m^4) |
|---------------|---|--------------------------------------|
| Blade's root | 1.765 | 4.837 |
| Tower base | 4.15 | 8.416 |

Using Eq. (7) and replacing the stresses with the corresponding load/moment amplitudes, Eq. (8) can be rewritten as Eq. (10).

$$295 \quad D = \left(\frac{c}{I_y}\right)^m \sum_{i=1}^{N_s} \frac{n_i Mx_i^m}{k} \quad (10)$$

The parameter M_i in Eq. (10) represents the load ~~(moment)/moment~~ ranges in the time series. We use Eq. (10) to estimate the ~~DEL~~ damage equivalent load (DEL), a parameter that we use in the current study to represent damage. The following section describes DEL.

2.4.1 Damage equivalent load

300 ~~DEL~~ Damage-equivalent load (DEL) is a tool to compare the damage ~~caused by different variable amplitude loading scenarios~~ caused by different variable amplitude loading scenarios. ~~Burton et al. (2011) define that two different loading scenarios with variable amplitude can cause. Burton et al. (2011) defines~~ Burton et al. (2011) defines DEL as the magnitude of the constant-amplitude load or stress causing the same damage as the ~~variable-amplitude~~ variable

amplitude loading with the same equivalent number of cycles (N_{eq}) causes. Equation (11) shows the mathematical expression of this definition based on Miner's rule (Eq. (10)).

$$305 \quad \frac{Neq(E[DEL_s^m])}{k} \left(\frac{c}{I_y} \frac{c}{I} \right)^m = \frac{\sum_{i=1}^{N_s} (n_i M x_i^m)}{k} \left(\frac{c}{I_y} \right)^m \frac{\sum_{i=1}^{N_s} (n_i M_i^m)}{k \left(\frac{c}{I} \right)^m} \quad (11)$$

In the above Eq. (11), DEL_s is the DEL of a sample of 10-minute time series containing N_s number of stress bins $\bar{\tau}$ and N_{eq} is the reference number of cycles. In the current study, we set N_{eq} equal to 951 cycles corresponding to the average number of cycles in a 10-minute interval based on the simulations of DTU the 10-MW-10MW turbine with DLC 1.2 condition and frequency of sampling equal to 100-load case conditions. Both sides of Eq. (11) represent the expectation of damage in a time span of 10 minutes. We use the expression on the right side to simplify the reliability assessment procedure and to be able to separate the variability of the load from material properties. Equations We use Eq. (12) and Eq. (13) are used to calculate the lifetime damage estimation ($DEL_{lifetime}$) from the 10-minute sample DEL estimations.

$$310 \quad E[(DEL_{bin})^m] = \sum_{s=1}^{SS} \frac{(DEL_s)^m}{SS} \quad (12)$$

In Eq. (12), SS is the number of 10-minute samples with the wind condition (same mean wind speed and turbulence (same wind condition)) but with different wind realizations (different turbulence seeds). Furthermore, DEL_{bin} is the DEL estimation in each wind condition (wind bin). In all current study cases, SS is equal to 6 samples bootstrapped from a database of 200 realizations (see Table 1).

$$E[DEL_{lifetime}^m] = \sum_{bin} E[(DEL_{bin})^m] P(bin) \quad (13)$$

In Eq. (13), $P(bin)$ corresponds to the joint probability of each wind condition (wind speed and turbulence). Since we are considering the marginal probability of turbulence conditioned on the mean wind speed bin, the joint probability equals the product is equal to the multiplication of the two marginal probabilities. Thus, Eq. (14) is another representation of Eq. (13).

$$E[DEL_{lifetime}^m] = \sum_{v_L=v_L}^{v_U} \sum_{t_L=t_L}^{t_U} E[(DEL_{bin})^m] P(T_{bin}|V_{bin}) P(V_{bin}) \quad (14)$$

In Eq. (14), the variables T_{bin} and V_{bin} represent the mean wind speed and turbulence in each wind bin $\bar{\tau}$ and $P(V_{bin})$ is the probability of occurrence of each mean wind speed (see Eq. (1)). In addition, the parameters v_L and v_U as well as t_L and t_U represent the lower bound and higher bound for mean wind speed and turbulence in each wind bin, respectively. Furthermore, $P(T_{bin}|V_{bin})$ is the conditional probability of each turbulence in each mean wind speed bin.

In study case 1 (constant turbulence), the probability of the representative turbulence value value of turbulence is assumed to be unity equal to 1. The following section presents the definition, mathematical relations, and procedure for estimating

2.4.2 Fatigue reliability assessment

Structural reliability is the ability of a structure to fulfill the structural design request for a defined period of time (ISO 2394, 2015). Equation (15) shows the probabilistic representation of this ability as a function of time.

$$R(t) = 1 - P_f(t) \quad (15)$$

335 In Eq. (15), $P_f(t)$ is the probability of failure at time t and can be stated as the probability of exceeding a certain level. Commonly, this problem is referred to with a function named limit state function ($g(x, t)$). ~~The and the~~ safe region is where ~~the limit state this~~ function is positive. In the design phase, the designer sets a level of reliability for the ~~end-of-the-design~~ lifelifetime, which accounts for an optimal balance among-between failure consequences, cost of operation and maintenance, material costs, and the probability of failure ~~tolerable-by-societies~~ (Sørensen, 2015). In the present work, we perform the

340 probabilistic reliability assessment by taking the following steps as described in (Madsen et al., 2006):

1. Modeling of limit state equation ~~$g(X)$~~ $g(X)$.
2. Quantification of uncertainties and modeling by stochastic variables ~~X~~ X .
3. Applying reliability methods to estimate the probability of failure (first-order reliability method in the current ~~cases~~ cases)

The limit state function in ~~assessing safety within the assessment of safety within at~~ time t can be written as Eq. (16).

$$345 \quad g(X, t) = R(X, t) - S(X, t) \quad (16)$$

In Eq. (16), R indicates the resistance of the component ~~r~~ and S is the loading. In addition, X represents a set of stochastic variables involved in each whose uncertainty propagates through the load and resistance. In the present study, we assess the reliability in time intervals of equal to 1 year ~~τ~~ and the time ~~remains would remain~~ constant through each reliability assessment. Thus, ~~from here on in the continuing~~, we eliminate t from the relations and notations ~~for simplification to simplify~~. Failure

350 occurs if the function g in Eq. (16) is smaller than or equal to zero. In other words, the probability of failure is the probability of the limit state function being equal to or less than zero. Accordingly, the probability of failure can be defined as Eq. (17).

$$P_f = \int_{\underline{g(x) \leq 0}} \mathbb{1}_{g(x) < 0} f_x(X) \quad (17)$$

Miner's rule does not consider the load sequence effect in variable loading and thus leads to errors in ~~fatigue damage prediction~~ the prediction of fatigue damage. There are some studies (Schaff and Davidson, 1997; Yanan et al., 1991; Rognin et al., 2009) showing high errors in the fatigue estimation of the composite materials, often in the form of overestimation, when

355 using Miner's rule. We account for the uncertainty in Miner's rule by defining the ~~damage limit~~ limit of damage as a random

variable with a mean value of 1 (Miner's rule limit for failure). With such an assumption, the limit state function for fatigue failure can be specified as Eq. (18) (~~Márquez-Domínguez and Sørensen, 2012~~)marquez2012fatigue.

$$g(X) = \Delta - D \quad (18)$$

360 In Eq. (18), Δ represents the fatigue limit in Miner's rule as a random variable with a mean value equal to unity. Using Eq. (11) for defining the damage, Eq. (18) can be rewritten as Eq. (19).

$$g(X) = \Delta - \frac{NeqDEL_{lifetime}^m}{k} \left(\frac{c}{I_y} \frac{c}{\tilde{I}} \right)^m \quad (19)$$

The limit state function in a specific time can be shown via different expressions other than the common form ~~of in~~ Eq. (18). Equation (20) presents one ~~such alternative of such alternatives~~ (Dimitrov, 2013). In the present work, we use Eq. (20) since it
365 facilitates the separation of the fatigue loads from the material properties ~~.In addition, the linearized version makes the~~ as well as the use of simple fatigue reliability estimation methods ~~possible~~ because of linearization.

$$G(X) = \log\left(\frac{R(X)}{S(X)}\right) \quad (20)$$

Combining ~~EqsEq.~~ (19) and (20), the limit state function in the current study ~~is expressed~~ would be as Eq. (21).

$$G(X) = \log(\Delta) - \log(Neq) - m \log\left(\frac{c}{I_y} \frac{c}{\tilde{I}}\right) + \log(k) - m \log(DEL_{lifetime}) \quad (21)$$

370 The parameters $\log(Neq)$ and ~~$m \log(\frac{c}{I_y})$~~ ~~$m \log(\frac{c}{\tilde{I}})$~~ in Eq. (20) are constants. Thus, ~~Eq. (20)~~ the above equation consists of three random parameters related to the linear damage accumulation model ($\log(\Delta)$), material ~~resistance~~ Resistance ($\log(k)$), and load ($\log(DEL_{lifetime})$).

~~To~~ In other to find the probability of failure, after defining the limit state function, the integration in Eq. (17) must be solved. This integration is hard to solve analytically ~~.There and thus, there~~ are established methods for estimating the
375 ~~integral's result~~ answer. Some of the commonly used methods are the first-order or second-order reliability methods or Monte Carlo (MC) simulations (see ~~Melehers and Beck (2018)~~ (Melchers and Beck, 2018) for further details about each method). ~~Veers (1990) showed~~ Veers (1990) shows that the probability of failure of a wind turbine blade joint with a design target life of 20 years can vary from 2.2% when using the second-order reliability method (SORM) to 1.8% when using FORM. ~~In addition,~~ Toft et al. (2011) showed the differences in the results of MC and FORM in the case of blades can be very different because
380 ~~of high nonlinearities in the case of higher fatigue exponents as in composites. We also observe the differences in the MC and FORM for two scenarios (see appendix), showing that in both high fatigue exponents and low probabilities of failure, FORM is less accurate. In the current work,~~ the first-order reliability method (FORM). However, since we have simplified the

formulation of the limit state function to a linear summation of the random variables ~~to decrease such errors. In addition, we are comparing different scenarios and are not interested in the absolute values. However, we investigate the highest probabilities of failure in the case of blade and tower (see appendix). We~~, we expect the first-order reliability method to be suitable for solving the problem and we validated it by comparing the results of one of the case scenarios using FORM and MC. Thus, we use the FORM in the current work for both reliability assessment and ~~for~~ defining the importance of the inputs. The next section contains more details about this method.

2.4.3 FORM and importance ranks

As stated in the previous subsection, the FORM is one of the ways to estimate the solution of the integration in Eq. (17). In this method, the problem of the limit state function being more or less than zero is redefined in the ~~standard normal~~ Standard Normal space. In other words, all the distributions of the random variables are transformed to ~~standard normal~~ Standard Normal distribution, and the expression of the limit state function is also transformed. In ~~the standard normal~~ Standard Normal space, the probability of failure problem will change into looking for an optimum design point (X^* or correspondingly U^* in the standard normal space) that lies on the curve of $g(U) = 0$ and has the minimum distance from the origin. The corresponding distance is known as the reliability index (β). The reliability index is commonly used as a measure of structural reliability (for more details about FORM ~~, see Melchers and Beck (2018)~~ see (Melchers and Beck, 2018)).

Equation (22) shows the relationship between the reliability index and the probability of failure (Gulvanessian et al., 2012).

$$\beta = -\Phi^{-1}(P_f) \quad (22)$$

The operator Φ^{-1} shown in Eq. (22) corresponds to the inverse ~~CDF~~ cumulative distribution function (CDF) of the standard normal distribution.

~~ISO 2394 (2015)~~ The ISO standard (ISO 2394 (2015)) presents the basic recommendation concerning a required reliability level in terms of the reliability index ~~in-related to~~ a certain reference time. The minimum required reliability index is known as target reliability. Based on (IEC 61400-1, 2005), a target value for the nominal failure probability for structural design for fatigue failure mode of the wind turbine components in a reference period of 1 year is ~~$5 \cdot 10^{-4}$ corresponding to $5e-4$~~ corresponding to a target reliability of $3.7 \cdot 10^{-3}$ according to Eq. (22). More specifically, Veldkamp (2007) performed a cost-benefit analysis and reported the optimal reliability level for the blade to be 2.7 (probability of failure of ~~$3.5 \cdot 10^{-3}$~~ $3.5e-3$) based on the analysis. In the present work, we study the sensitivity of reliability to different variables and not the levels. However, we ~~also~~ present the reliability levels in different ~~study cases~~ cases of the study as well. We consider $R = 10$ for fatigue properties of the composite (Mikkelsen, 2020).

~~To~~ In order to apply FORM analysis, ~~we first~~ first, we fit distributions to the estimations of $\log(DEL_{lifetime})$ ~~obtained from bootstrapping and calculated via~~ calculated based on 10-minute simulations using Eq. (14) ~~based on 10-minute simulations~~. It

415 is more realistic to assume that different materials will have a different range of Δ because of differences in the scatter of the
strength data ~~, which will, in turn, which will in turn~~ result in different distribution parameters (Le and Peterson, 1999). We
gather and ~~reuse-re-use~~ the information about the distributions and statistical parameters of the material and Miner's rule limit
from the literature. Since the DTU 10-MW turbine is not designed against fatigue, we observed ~~low-reliability-low-reliability~~
levels in the blade root and the tower base (failure occurrence in the tower base). ~~To lower the errors in FORM in the case of~~
420 ~~the blade (high fatigue exponent and thus high nonlinearity), we calibrate the material strength towards low probabilities of~~
~~failure for the sake of accuracy.~~ Thus, in the current study, we increase the material fatigue strength proportional to the high
fatigue loads while keeping the corresponding coefficient of variation (CoV) the same as ~~for~~ real material to avoid effects on
the sensitivity analysis. These changes will affect our reliability levels. However, the main interest in the current study is the
sensitivities and changes, not the values. Table 3 shows ~~the distribution parameters~~ this information plus the references for the
425 coefficients of variation.

Table 3. Characteristics of the material and model variables

| Variable | Component | Distribution | Mean <u>mean</u> | Standard Deviation <u>std</u> | Reference |
|----------------|-----------|--------------|-----------------------------|--|--|
| $\log(\Delta)$ | blade | Normal | -0.1116 | 0.4724 | (Toft and Sørensen, 2011; Stensgaard et al. |
| | tower | Normal | -0.0431 | 0.2936 | (Stensgaard et al., 2016b) |
| $\log(K)$ | blade | Normal | calibrated | 0.528 <u>0.602</u> | (Mortensen et al., 2023; Toft and Sørensen |
| | tower | Normal | calibrated | 0.2 | (Sørensen, 2015; Slot et al., 2019; Toft and Sørensen, 2011) (S |

~~We would like to see the sensitivity of fatigue reliability to changes in fatigue loads in addition to material strength. Different
materials (used in different components) have different fatigue exponents, and thus the effect of change in their loading on
reliability can be different (the higher the fatigue exponent, the higher the effects of loads in the overall damage and reliability).~~
430 ~~We want to take this fact into account while being consistent in the idea of the variability of k . Thus, we consider k as the
variable representing material uncertainty and redo the assessments in three different levels of m in each load channel under
study. We calibrate the initial reliability in the annual reliability assessments in case I to avoid misinformation due to the
correlation between m and k . The linearized formulation of the limit state function makes this separation easier by showing
the m on the load site.~~

435 After specifying all the distributions and probabilistic parameters of each random variable in Eq. (21), we transform each
~~non-normal distribution to normal using the normal tail~~ non-Normal distribution to Normal using the Normal tail approxima-
tion and Rackwitz-Fiessler algorithm (Rackwitz and Fiessler, 1978) to find the optimum design point. The following contains
the relations and procedures for the transformation and solving procedures.

In transforming ~~non-normal of non-Normal~~ continuous distributions to standard normal Normal, since the design points (X^*)
440 are usually located at the tail of the ~~standard normal~~ corresponding Normal distribution, we estimate the corresponding mean
 $\mu_{x_i^*}$ and standard deviation $\sigma_{x_i^*}$ based on the design point x_i^* using Eq. (23) and Eq. (24), respectively (Rackwitz, 2007).

$$\sigma_{x_i^*} = \frac{\phi(u_i^*)}{f(x_i^*)} \quad (23)$$

$$\mu_{x_i^*} = x_i^* - \sigma_{x_i^*} u_i^* \quad (24)$$

In Eq. (23) and Eq. (24), the operator ϕ is the ~~CDF of standard normal distribution~~, cumulative distribution function (CDF)
 445 of standard Normal distribution and f corresponds to the PDF of the initial ~~non-normal-non-Normal~~ distribution. In addition,
 x_i^* is the non-normally distributed random variable in the design point (X^*), and u_i^* is the corresponding element in the design
 point in the standard normal space (U^*). u_i^* is acquired as Eq. (25).

$$u_i^* = \Phi^{-1}(F(x_i^*)) \quad (25)$$

F in Eq. (25) stands for the CDF of the point in the initial distribution. In fact, Eq. (25) presents the basic concept that in the
 450 transformation process between different distributions, the probability of each point remains unvaried.

This method also provides information ~~regarding the relative importance~~ regards the importance level of each random vari-
 able or, in other words, the sensitivity of the output (~~reliability~~) to each input. A vector α provides such information: ~~α is a~~
~~unit vector defining the position of u_* (the design point) and β is its magnitude. Equation (26) shows the expression.~~ Eq. (26)
and Eq. (27) show the expressions for this vector ~~and~~ and the importance factor of each parameter based upon.

$$455 \quad \alpha = -\frac{\nabla g(u^*)}{|\nabla g(u^*)|} = \frac{u^*}{\beta} \quad (26)$$

~~The problem is solved in an n dimension space in which each dimension represents the values of one random variable. Thus,
 the unit vector α is composed of each variable's normalized magnitude in the design point. These normalized values define the
 share of each variable in defining the position of the design point. Therefore, the relative importance of the variables (known
 as the importance rank) can be shown by a factor as shown in Eq. (27).~~

$$460 \quad \text{Importance factor} = \frac{\alpha_i}{|\alpha|} \quad (27)$$

~~In Eq. (27), as~~ Since α is a unit vector, the denominator in Eq. (27) is equal to one, and thus, α_i is the importance factor for
 variable x_i .

~~The failure probability at each point in time (year in this case) depends on the survival at the previous point (one year before)
 . Thus, the annual reliability is useful for assessing the probability of failure at the end of each year. The Eq. (28) and Eq. (29)~~
 465 present the formulation for calculating the annual probability of failure in time t conditional on survival in time $(t - \Delta t)$ is a
~~special case of conditional probability. The corresponding posterior probability is shown in Eq. (28).~~

$$\Delta P_f(X, t) = \frac{P(X, t - \Delta t \leq f \leq t)}{P(X, f > t - \Delta t)} = \frac{P_f(X, t) - P_f(X, t - \Delta t)}{(1 - P_f(X, t))}$$

Using Eq. (22), the corresponding and an annual reliability index is as in Eq. (29). (Velarde et al., 2019).

$$\Delta P_f(X, t) = \frac{P_f(X, t + \Delta t) - P_f(X, t)}{(1 - P_f(X, t))\Delta t} \quad (28)$$

470

$$\Delta \beta(X, t) = -\Phi^{-1}(\Delta P_f(X, t)) \quad (29)$$

2.4.4 Sampling

To fit the distributions to DEL data in different case studies, we need to sample from the turbulence distribution in each wind speed bin to account for turbulence probability (see Eq. (14)). For sampling turbulence levels from cases 2 and 3, we divide their corresponding probability space into 5% probability intervals, and then we consider take the median of each probability interval as the representative. We derive the corresponding turbulence sampling point by taking the inverse of the CDF at the median point. Following such an approach, the samples we can account for all probability levels equally. The probability of each sampling point is equal to 5%. Fig. 3 shows the resulting sampling points in different mean wind speeds.

480 ~~Figure~~

~~Fig. 3~~ reveals that the turbulence levels within the same probability are higher in case 2 (lognormal distribution) compared to case 3 (Weibull distribution) below 90% quantile. The trend changes above 90% quantile. The differences are higher in the higher turbulence levels with lower probability, especially, in higher mean wind speeds.

The following section provides the results of the study.

485 3 Results and discussions

The current section presents the results of the study in two steps. First, we introduce the distributions of DEL in different turbulence modeling cases in Sect. 3.1. Then, in Sect. 3.2, we investigate the change of fatigue reliability through time in different turbulence modeling approaches models and in different Wöhler curve exponents in Sect. 3.2. Sect. 3.3 contains the sensitivity analysis of the reliability to changes in random inputs in of each input in different scenarios. Sect. 3.4 investigates the effects of the design class on the overall results of the previous sections. Finally, Sect. ??-3.4 includes supplementary discussions about the results. All the results are provided for both the blade root flapwise and tower base fore-aft load channels.

490



Figure 3. Sampling points of turbulence within intervals of size 0.05 in the corresponding in case 2 (lognormal distribution) and case 3 (Weibull distribution) ~~at five different mean wind speeds~~

3.1 Probability distributions and statistical parameters of load

Wind ~~speed~~ fluctuation is one of the main causes of fatigue damage, especially in the load channels like the blade flapwise and tower ~~base~~ fore-aft. ~~A~~ Thus, if we set the mean stress level constant, the higher load fluctuations (higher standard deviation in the loads) cause higher fatigue damage in the components. Therefore, a change in the wind standard deviation (turbulence) in each mean wind speed level directly changes the estimated fatigue damage. In the current section, we look into the change in the distribution of DEL with the change in turbulence characterization ~~approach-method~~ in the IEC ~~NTM~~ Normal Turbulence Model. In case 1, each realization of DEL_{bin} is based on one turbulence level (representative turbulence) ~~;~~ while in the other two ~~case studies, it~~ cases (considering lognormal and Weibull distributions for turbulence), each realization is a result of integration over all 20 turbulence levels ~~sampled from lognormal and Weibull distributions~~ each represented via one realization.

Figure Fig. 4 shows DEL_{bin} values ~~averaged over all seeds in each turbulence level resulting from different turbulence levels and seeds using~~ (Eq. (12)–(12)) in cases 2 and 3. ~~Figure Fig. 4 only contains the fatigue exponent considered in the design, which is equal to 10 in the blade root and equal to 3 in the tower base.~~

505 The bar plots of Fig. 4 show the binning over mean wind speeds and turbulence levels ~~we sample with equal probability over the domain~~. It reveals the increase of the DEL with an increase in ~~the~~ mean wind speed and standard deviation of the wind. The only exception to this trend is the DEL in the tower base around mean wind speeds of 6 m/s and 8 m/s. The reason is that around these mean wind speeds, there is a local peak in DEL values ~~due to because of the~~ resonance (Mozafari et al., 2023).

Another observation from Fig. 4 is the relatively ~~fast faster~~ decrease of the ~~tower-base~~ DEL_{bin} ~~in tower base~~ as a function of turbulence compared to the blade. ~~In other words, the difference between $DEL_{lifetime}$ obtained from a single high turbulence level and a single low level is relatively higher in the tower base. This is partly because of the resonance in the tower (see Mozafari et al. (2023)), which enhances the effect of turbulence level on fatigue loads. This observation reveals that the variability in the case of the tower base is much higher in each wind bin (check (Mozafari et al., 2023) for more details).~~ Thus, we expect the integration over all turbulence levels (see Eq. (14)) to be more effective in decreasing variability in ~~tower base~~ DEL_{bin} ~~in the tower case. As a result and thus,~~ $DEL_{lifetime}$ estimations ~~in the case of the tower base would also show lower variability.~~ The following includes observations on $DEL_{lifetime}$ distributions.

510
515

Using the 200 samples in each wind bin (consisting of constant turbulence and constant mean wind speed), we calculate the $DEL_{lifetime}$ using Eq. (13) in case 1 (constant 90% turbulence) and Eq. (14) in cases 2 and 3 (lognormal and Weibull distribution). We ~~use a samples size of six (recommended number of samples by the IEC 61400-1) from the database and repeat take samples of size 6 from this database~~ 1000 times with replacement (bootstrapping) to obtain the distributions of ~~DEL when following IEC recommendations regarding the number of sample sizes. This method results in 1000 $DEL_{lifetime}$.Figure realizations in each case.~~ Fig. 5 shows the probability density function (PDF) of the $DEL_{lifetime}$ estimations in different turbulence cases and different fatigue exponents in both load channels under study. The results are all normalized by the mean ~~$DEL_{lifetime}$ in case 1. of the Case 1 data in each condition.~~

520
525

Fig. 5 reveals that the overall variability of the $DEL_{lifetime}$ realizations are higher in the case of the tower base compared to the blade root, as expected due to the reasons discussed above and in (Mozafari et al., 2023). This remains the case for all ~~approaches methods~~ of turbulence modeling. The distributions are not significantly impacted by the fatigue exponent, as indicated by the similarity of the distributions in the different rows ~~of Fig. 5.~~

530

Based on Fig. 5, the integration over turbulence distributions (cases 2 and 3) instead of using one representative value (case 1) ~~decreases not only not only decreases~~ the mean value but also the variance of the realizations. This effect is more notable in the case of the tower base. This is expected, as Fig. 4 shows that the variability in the tower base DEL_{bin} is larger than in the blade-root moment. The lower variance of the $DEL_{lifetime}$ realizations is partly because ~~we do one extra integration step in~~ the calculations of this parameter in cases 2 and 3 ~~(see (Mozafari et al., 2023) to see the effect of summation on the variability in case 1). The integration over the whole range results in an expected value, which is more robust than a single value (90% we~~

535

./Figures/Fig3.pdf

Figure 4. DEL_{bin} in each mean wind speed and turbulence level (wind bin) in a) case 2 (turbulence sampled from Turbulence sampling based on lognormal distribution) for blade root ; b) case 2 for the tower base ; c) case 3 (turbulence sampled from Turbulence sampling based on Weibull distribution) for blade ; and d) case 3 for tower base (the The results are only shown for comparison and the DEL dimensions are relative)

do one extra step of integration. The other reason is considering lower turbulence levels instead of focusing on the upper tail

./Figures/Fig4.pdf

Figure 5. Probability density function (PDF) of normalized and the best distribution fits to DEL estimates using 1000 bootstrap samples of size 6 in different turbulence study cases based on a) blade root flapwise ($m=8$), $m=8$ b) blade root flapwise ($m=10$), $m=10$ c) a) blade root flapwise ($m=12$), $m=12$ e) tower base fore-aft ($m=3$), f) tower base fore-aft ($m=4$), g) tower base fore-aft ($m=5$) of the distribution (90% quantile in this case).

540 Comparing the distributions of $DEL_{lifetime}$ in case 2 (lognormal) and case 3 (Weibull) in Fig. 5 reveals that the mean levels in case 2 are lower than in case 3. In other words, ~~estimating the estimation of~~ $DEL_{lifetime}$ based on the Weibull distribution of turbulence is less conservative ~~than compared to~~ the lognormal distribution approach. This complies well with the expectations based on the characteristics of the two distributions discussed in Sect. 2.4.4. The bias in the mean value of $DEL_{lifetime}$ calculated with the Weibull/lognormal distributions is more significant for the tower base than the blade root. ~~Thus; thus,~~ using representative turbulence is ~~relatively more conservative than the other approaches~~ ~~much more conservative~~ in the case of the tower base. For example, ~~for a in the case of the~~ tower with a fatigue exponent of 3, the $DEL_{lifetime}$ estimation can vary by more than 35% when using ~~six turbulence~~ ~~6~~ seeds.

~~Although the Weibull distribution of turbulence generally results in lower DEL estimations, there~~ ~~There~~ is an overlap between distributions of all cases in the blade root. ~~There is also an overlap and~~ between cases 2 and 3 in the tower base. This means if the designer uses only ~~six~~ ~~6~~ realizations, there is a chance that the $DEL_{lifetime}$ estimation using ~~the~~ Weibull distribution is more conservative than the lognormal. For example, ~~in~~ the tower base with a fatigue exponent of 5, $DEL_{lifetime}$ estimations in case 3 can be around 5-7% ~~%~~ more conservative than ~~in~~ case 2. In addition, ~~when using six seeds~~ in the blade root, ~~when using 6 seeds,~~ lognormal can provide a less conservative DEL estimation than the ~~90% 90%~~ turbulence level model. 555 Although such occurrences are ~~very~~ rare, the chances increase with an increase in the fatigue exponent in each load channel.

The general conservatism of using a ~~90% 90%~~ turbulence level in the DEL evaluations can show itself in the fatigue reliability estimations. In addition, since changing the method of modeling the turbulence changes ~~the both the mean and~~ standard deviation of the DEL realizations, the sensitivity of the reliability levels to the DEL ~~changes can also vary~~ ~~can also differ~~ from one case to another. We study the extent of such ~~an effect in different fatigue exponents and in different effect and the change in that with the change in fatigue exponent in the two~~ load channels in the next subsections.

3.2 Fatigue reliability in different cases

In the reliability assessments, we use the $\log(DEL_{lifetime})$ as the parameter representing the ~~fatigue~~ load (see Eq. (21)). ~~We must~~ ~~To complete the reliability analysis, we need to~~ determine an appropriate probability distribution for the load parameter ~~to complete the reliability analysis~~. Thus, we first find the probability distributions of $\log(DEL_{lifetime})$ in different conditions (each condition includes a load channel, a ~~normal turbulence modeling approach~~ ~~turbulence modeling case~~, and a specific fatigue exponent). Tables 4 and 5 represent some of the best distribution fits to the $\log(DEL_{lifetime})$ data and their parameters in three different turbulence model cases in $m = 10$ and $m = 3$ for the blade root and tower base, respectively (for more cases see appendix). ~~The trial of different distributions (GEV, lognormal, normal, and Weibull in this case) with the maximum likelihood method finds the best distribution for fitting in the current study.~~ 570

Using the distributions of $\log(DEL_{lifetime})$ and the distributions of other parameters ($\log(\Delta)$ and ~~$\log(k)$~~ ~~$\log(K)$~~) as we previously defined in Table 3, we estimate the annual reliability and its change through the lifetime (see Eq. (29) and Eq. (28)). It should be noted that although we derive different distributions of $\log(DEL_{lifetime})$ in the case of different Wöhler

Table 4. Best distribution fits to $\text{Log}(DEL_{lifetime})$ in different turbulence modeling cases considering flapwise bending moments in the blade root ($m = 10$)

| Case number | Distribution | Par 1 | Par 2 | Par 3 |
|-------------------------------|--------------------------|--------|-------|-------|
| 1 (Representative turbulence) | GEV (μ, σ, ξ) | -0.299 | 0.012 | 2.405 |
| 2 (lognormal turbulence) | GEV (μ, σ, ξ) | -0.239 | 0.006 | 2.349 |
| 3 (Weibull turbulence) | Normal (μ, σ) | 2.323 | 0.007 | - |

Table 5. Best distribution fits to $\text{Log}(DEL_{lifetime})$ in different turbulence modeling cases considering fore-aft bending moments in the tower base ($m = 3$)

| Case number | Distribution | Par 1 | par 2 | par 3 |
|-------------------------------|---------------------------|-------|-------|-------|
| 1 (Representative turbulence) | lognormal (μ, σ) | 1.11 | 0.01 | - |
| 2 (lognormal turbulence) | Normal (μ, σ) | 2.824 | 0.012 | - |
| 3 (Weibull turbulence) | GEV (μ, σ, ξ) | -0.22 | 0.01 | 2.73 |

exponents, the distributions in [Table 3](#) only refer to the reference levels of this exponent in the design. For
 575 Thus, for the sake of comparison of the trends, we modify the mean value of $\log(k) \cdot \log(K)$ in different variations of fatigue
 exponents ($m = 4, m = 5$ for the tower and $m = 8, m = 12$ for the blade) such in a way that we get the same reliability level in
 the first year in case 1. The modification sets a benchmark for comparison. Figure 6 shows the reliability change
 of reliability over 20 years in the blade root and the tower base in different conditions.

The results in Fig. 6 show that the in both load channels and in different fatigue exponents, constant turbulence (black lines)
 580 provides conservative annual reliability levels results in terms of annual reliability level. The next conservative evaluation be-
 longs to the lognormal distribution lognormal (blue lines) and the last to the Weibull distribution Weibull (red lines). The ranks
 remain the same in all cases. In other words, the overlaps in the distributions of $DEL_{lifetime}$ DEL observed in Fig. 5 between
 cases 2 and 3 are not seen in Fig. 6 and do not affect the reliability trends. We explain the reason in the sensitivity analysis
 presented in the next section.

585

In general, the tower base shows a very fast reduction in reliability over time. One possible reason is the high higher mean
 value of the $\log(DEL_{lifetime})$ versus especially versus material fatigue resistance ($\log(k) \cdot \log(K)$) in this load channel. We
 are using the conventional method of linearly linear scaling the damage with time. This In a high DEL magnitude, this
 leads to a fast increase in damage over time in a high DEL magnitude.

590

In the case of constant turbulence in the tower base, the change in the fatigue exponent (m in 'm') has a more visible effect on
 the rate of reliability declination through time. In this case, a larger m in 'm' increases the decline in reliability level from the
 same initial point at year 2.

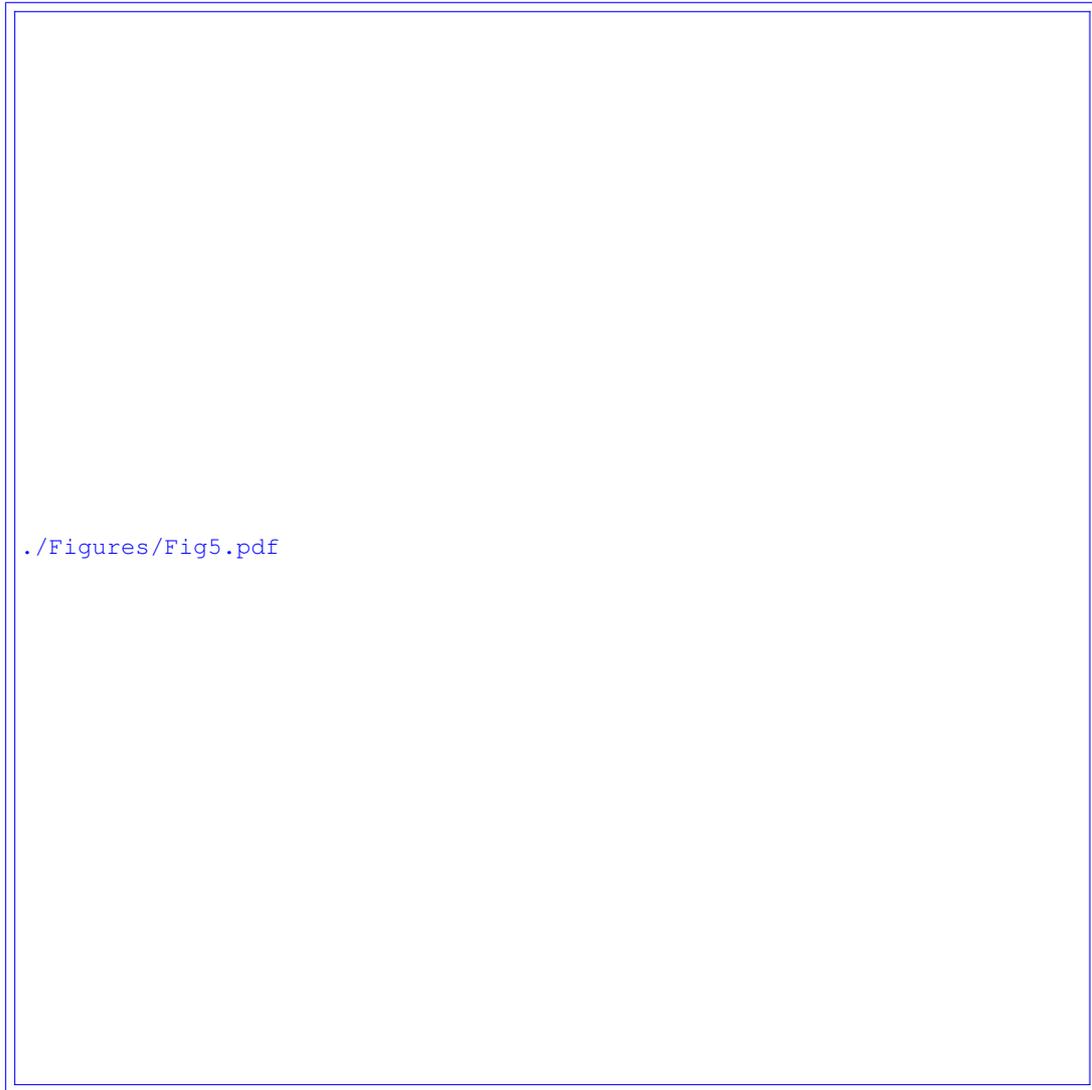


Figure 6. Reliability index through the lifetime ~~considering in~~ a) ~~bladeroot's~~ flapwise and b) tower base fore-aft ~~moments-load channels~~ in cases 1, 2, and 3 considering different Wöhler exponents

595 Notice that the ~~difference in the results~~ results seen in the tower base are more visible because of the higher initial variability in the DEL in this load channel. In the case of the blade, the same trends occur ~~;~~ but they are less visible.

3.3 Importance ranks of the inputs

We study the sensitivity of the reliability level at ~~year-20 to each random input to~~ years to each of the random inputs in the
600 limit state function. The importance rank of each of the inputs is derived ~~from~~ based on FORM analysis (see Eq. (27)). **Figure**

7 and Fig. 8 show the ~~The~~ relative importance levels in different cases and fatigue exponents are shown in Fig. 7 and Fig. 8 for the blade root and tower base, respectively. ~~In~~ It should be noted that in these plots, the extent of differences ~~does not represent the absolute sensitivity to~~ is not representative of the absolute importance of the load, material fatigue strength, and Miner's rule ~~but their relative importance. The reason is that the random inputs to the model are in logarithm scale and showing a different CoV for each variable. The~~ we model the logarithm of each of the variables, and the levels of magnitude are very different. However, they show relative importance in terms of rank. In addition, the change in the percentages from one case scenario to another is still a good measure for comparing ~~sensitivity of the reliability to each source of~~ sources of uncertainty and tracking changes ~~with change of scenarios~~ in the sensitivities.

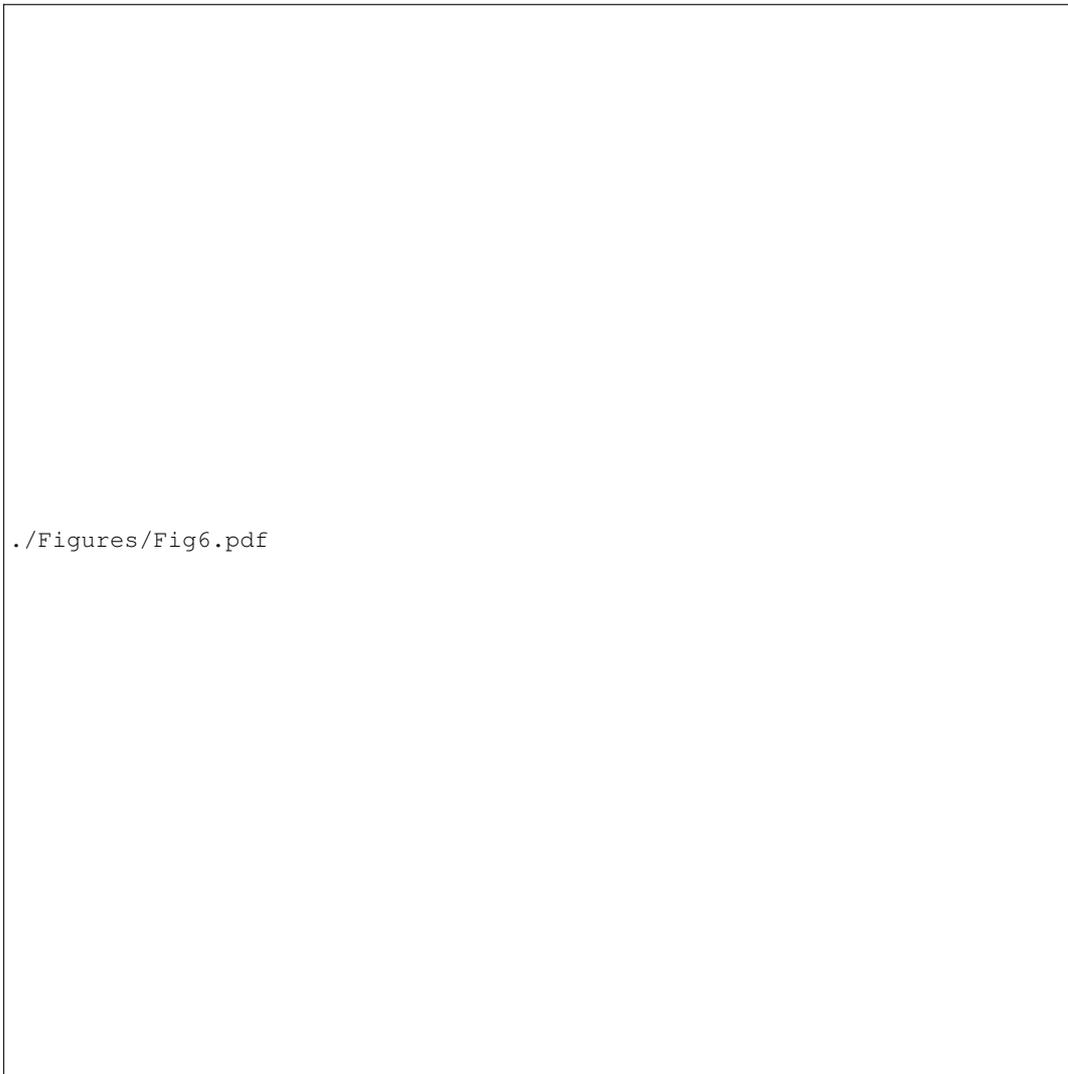


Figure 7. Importance factors of different random inputs in assessing annual reliability level at year 20 in blade's flapwise load channel in cases 1, 2, and 3 considering different Wöhler exponents

Figure Fig. 7 shows the relatively high importance of the fatigue resistance of the material in the ~~case of the~~ blade root. The second ~~importance belongs to important parameter is~~ the uncertainty in ~~the~~ fatigue accumulation model. ~~The relative effects of the two~~ Their relative effects are much higher than the loads because of the low variance of load in the blade. The lower variance in the DEL when using integration over turbulence in each wind speed bin (as shown before in Fig. 5) decreases the effect of this parameter on the reliability level. The share of the ~~logarithm of~~ load in the overall reliability increases with the increase of fatigue exponent γ , as we expect. However, the importance of the load uncertainty compared to the other two parameters is negligible ~~in all cases~~.

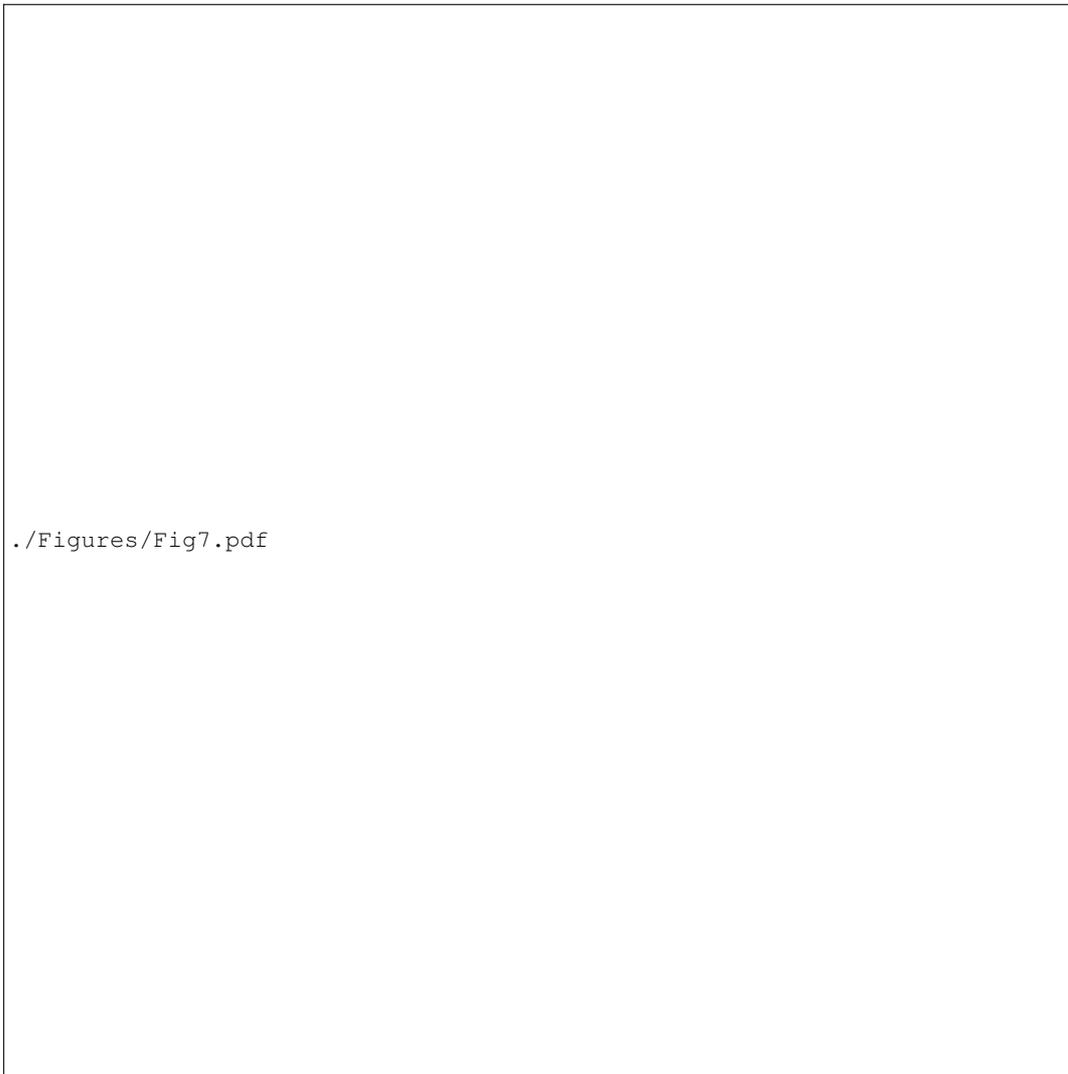


Figure 8. Importance factors of different random inputs in assessing annual reliability level at year 20 in tower base fore-aft load channel in cases 1, 2, and 3 considering different Wöhler exponents

Figure 8 shows the relative high importance of the Miner's rule uncertainty as the coefficient of variation in $\log(k)$ in steel (material in the tower base) is much lower than in the composite (in the blade). The second effective parameter is the fatigue resistance of the material K , and the load is the least important part of the uncertainty in the reliability.

620 The effects of the fatigue loads on the reliability in the tower base are relatively higher than in the case of the blade root (see Fig. 7). This is because of the higher CoV in the fatigue loads in the tower base.

As seen in the previous load channel (blade root flapwise), we observe an increase in the importance of the loads with an increase in the fatigue exponent. In addition, the case 2 and 3 turbulence modeling decrease the CoV of $\log(DEL_{lifetime})$ and thus its importance in fatigue reliability.

According to both Fig. 7 and Fig. 8, there is no obvious change in the importance factors when changing the distribution from lognormal to Weibull. In other words, the change in CoV of DEL is very low when changing the distribution of turbulence. It must be emphasized again that the differences are exaggerated since the input parameters are in logarithmic scale; however, the relative importance is valid and reliable.

3.4 Effects of wind turbine design class Overall discussions

The thickness of the tail in the lognormal distribution is dependent on its standard deviation. The standard deviation of the distribution in different cases of NTM is a function of the reference turbulence level (see Eq. (2) to Eq. (6)). This means that there is a possibility that the results of the current study change with the wind turbine class. One case of lower reference turbulence intensity equal to 0.1 is tested in the current study showing the same trends. Figure ?? shows the distributions of $DEL_{lifetime}$ in three different cases of the study for $I_{ref} = 0.1$ for two of the scenarios (tower base, $m = 3$ and blade, $m = 12$).

Different distributions of $DEL_{lifetime}$ in two example cases of a) blade, $m = 10$ and b) Tower, $m = 4$ for $I_{ref} = 0.1$ considering different editions of normal turbulence model

In forming the distribution of the wind speed (using the Weibull distribution shown in Eq. (1)), the annual mean wind speed defines the scale factor of the Weibull distribution. The scale factor in the Weibull distribution directly affects the standard deviation. Thus, there might be a change in the overlaps of different fatigue load data with a change in the class of the annual mean wind speeds. We study this effect via some examples with different mean wind speeds in two different reference turbulence intensities to cover some design classes. Figure ?? presents the results for one case with the highest possibility of overlap (high fatigue exponent).

$DEL_{lifetime}$ probability distributions using different editions of NTM in different annual hub-height mean wind speed and reference turbulence intensity considering blade root flapwise moments, $m = 12$

Figure ?? reveals that with a decrease in the annual mean wind speed, the overlap between the DEL distributions resulted from different NTM case increases. As an example, there is a visible overlap between the long-term fatigue load distributions in the case of using representative turbulence and using full Weibull distribution. This means that in design classes with very low mean wind speed, when using six turbulence realizations, the designer can possibly get more conservative results from following edition 4 NTM versus edition 1 of the IEC standard.

According to Fig. ??, there is no obvious mutual effects from changing both representative turbulence and mean wind speed, while the changes due to the change in the mean wind speed are more obvious. To make sure that there is no such consideration in the case of the tower with the highest m results ($m = 5$), this case is investigated with low reference turbulence and low annual mean wind speed. Figure ?? shows the corresponding results.

~~$DEL_{lifetime}$ probability distribution obtained from using different editions of normal turbulence model in annual hub-height mean wind speed of 5 m/s and reference turbulence intensity of 0.1 considering tower base fore-aft moments, $m = 5$. As Fig. ?? shows, there is no considerable overlap in the case of the tower at the extreme end of case study design classes.~~

660 To investigate the effects of the design class on the annual reliability, two of the cases for the blade with $m = 12$ are compared in Fig. ??.

Different distributions of $DEL_{lifetime}$ in two example cases of blade, $m = 12$ in two annual average mean wind speeds of 5 m/s and 7.5 m/s considering different editions of NTM

665 The results presented in Fig. ?? show a higher difference between the annual reliability level at the end of the design life in an IEC design class with a lower annual mean wind speed. In such classes, although the mean levels get closer between case 1 and case 3, the higher variability in case 3 decreases the corresponding reliability level when using a probabilistic approach. It is important to consider this difference in case of any further calibration of the safety factors in future versions of the standard.

3.5 Overall discussions

670 The results (especially in Fig. 6) reveal the high effect importance of the fatigue exponent in reliability estimations considering tower base fore-aft moments due to the relatively high magnitude of the fatigue load in this load channel the tower base in design-level reliability estimations. The fatigue strength curves of the steel structures are normally bilinear. The bi-linear and the selection of the fatigue exponent at the design level ,when using damage equivalent loads, especially when using equivalent forms like DEL can vary between the lower, the higher, or the average slope of the actual S-N curve. The results in the current work elaborate on the effect of the selection importance of focusing on the characterization of the steel fatigue exponent at the 675 design level ,as the annual reliability levels of the tower base (normally experiencing high loads) can be are very sensitive to this parameter.

~~In addition, the~~ The results of reliability estimations show that the small overlaps seen in the DEL distributions are not very important when coming into the reliability framework. This has been made clearer more clear in the sensitivity analysis, ~~where~~ 680 ~~the effects of load variations are shown to be relatively~~.

A potential concern with the results is the difference in sample size for the different cases. In particular, there are more 10-minute simulations involved in estimations in cases 2 and 3. A larger sample size naturally decreases the variance in the $DEL_{lifetime}$ evaluations due to the law of large numbers (see (Mozafari et al., 2023) for more details). To investigate whether 685 this is significant, we checked the effect by using different combinations of seed numbers and the corresponding effect on the trends is negligible.

Since the distributions in the IEC standard NTM are functions of parameters for each class of wind turbine (see Eq. (2) to Eq. (6)), the results depend on the class. We re-performed the study for a lower reference turbulence intensity more suitable for

690 offshore cases (0.1) and the trends were the same in terms of DEL distribution biases. However, we encourage similar studies on different classes of wind turbines to track the possible differences in terms of magnitudes.

All in all, although the choice of the turbulence characterization approach impacts the reliability and the sensitivity of the reliability to different uncertainty sources, these effects are not notable when compared to the high sensitivity of the reliability to other sources in every case. In other words, accurate modeling of the damage accumulation or more accurate characterization of the material properties (especially in the case of composites) can impact the reliability levels to a relatively-much higher extent. ~~There is a Considering the~~ 50% change in the reliability level at year 20 in the case of the tower base with $m = 5$ ~~with change in the loads. Considering the higher effect of the changes, and the fact that the uncertainty~~ in the material properties, ~~the effects of uncertainty in this random variable on reliability in this case has around 8 times higher impact than load, the changes~~ can be drastic.

700 There are also some limitations ~~and potential for extension of the study. The most important assumptions that can limit the generality of the results are as below:-~~

~~Reference turbulence intensity (design class of the wind turbine): The to consider when using the results of the current study. For example, the~~ thickness of the tail in the lognormal distribution ~~depends is dependent~~ on its standard deviation ~~;-The standard deviation of the distribution which~~ in different cases of NTM, is a function of the reference turbulence level (see Eq. (2) to Eq. (6)) ~~in each mean wind speed.~~ This means that there is a possibility that the results of the current study change with the wind turbine class. ~~Some examples are tested in the present study. However, we encourage similar studies on other classes of wind turbines to track the possible differences in the trends and results. In addition, the annual mean wind speed influences the variability of the long-term fatigue loads, and thus overlaps between different study cases. We suggest further studies on the lower mean wind speeds and the combination of the class with other changes. Therefore it is valuable to investigate the case of~~

705 lower reference turbulence levels to come to general conclusions.

~~Additional averaging of data in case of full distributions: A potential concern with the results is the difference in sample size for the different cases. There are more 10-minute simulations involved in estimations in cases 2 and 3. A larger sample size naturally decreases the variance in the $DEL_{lifetime}$ evaluations due to the law of large numbers (see (Mozafari et al., 2023) for more details). To investigate whether this is significant, we checked the effect by using different combinations of seed numbers, and the corresponding effect on the trends is negligible. However, we encourage testing of different calculation approaches to track any possible changes in the variability of fatigue loads in cases of using full distributions of the turbulence--~~

715

~~Other load cases: Among the standard design load cases related to fatigue, idling, and power production with fault also include the NTM in the IEC standard. It is valuable to perform the same study considering these other load cases and their corresponding probabilities. In addition, considering all relevant load cases for fatigue (including shutdowns and start-ups) can change the long-term fatigue distributions and trends and should be considered in future studies.~~

720

~~Specificity of the wind turbine response: The main study uses the DTU 10-MW wind turbine as the case study. The size and design of the wind turbine and its controller's design affect the turbine's response to a specific wind input. The Siemens~~

725 2.3-MW wind turbine (with a smaller size) but a similar controller and class is checked, and the results show the same trends in distributions of the long-term fatigue load. In future studies, testing other wind turbines with a different type of controller and also using other aeroelastic simulation tools is beneficial.

Variability of the material properties and damage accumulation rule: The variability of the initial material fatigue strength and Miner's rule are taken from the literature. Updating the corresponding coefficients of variations can change the levels in the sensitivity analysis.

730 Variability of the fatigue loads: The only variable considered in defining the fatigue loads is the variation in the turbulence inputs. While the shares of load uncertainty due to this specific variation are covered, the sensitivity results can vary when considering other sources of uncertainty in the loads.

735 Method of reliability assessment: The first-order reliability method performs well in very low probabilities of failure and less accurately in higher failure probabilities. In addition, doing the same reliability analysis using MC-Monte Carlo instead of FORM can provide more accurate reliability estimates if computational resources are available (see appendix for a detailed explanation regarding computational expenses of MC) in the case of having computational resources.

Offshore versus onshore: The study uses aeroelastic simulations with only onshore wind inputs. However, in the offshore cases, the effects of wind turbulence on the structure response varies. The effect is more in the case of tower loads. We recommend performing the same study for offshore cases to investigate the possible changes in the trends.

740 4 Conclusions

The assessment of the remaining fatigue lifetime hinges upon reanalyzing the the re-analysis of the reliability. In performing such an analysis per the IEC standards, a designer can choose to follow different recommendations regarding probabilistic modeling of the turbulence. The in the IEC standards regarding characterizing turbulence, but the ramifications of those choices are currently unclear. For example, as the present study shows, using six shown by the current study, using 6 realizations for the estimation of DEL, in the case of the tower with a fatigue exponent of 3, the estimations based on DEL estimation based on case 3 (the Weibull distribution of turbulence) can differ by 40% from the representative turbulence approach. Regarding case. In addition, the annual reliability index after 20 years can differ by a factor of two (with Weibull distribution being less conservative). In terms of fatigue reliability at the end of the design life-lifetime (20 years), the differences are up to 50% in the case of the blade root and up to 200% in the case of the tower base. Such-This high difference can change the possible scenarios at the lifetime extension stage and must be considered. The difference in reliability levels varies with a change in the design class. Consideration of the difference between classes is important in case of any further calibration of the safety factors in future versions of the standard. taken into consideration.

750 The results presented in this paper are very applicable to the wind turbine design stage .The study informs the designer as they provide the designer with information about the extent to which following different editions of the IEC standard can change the expected value and uncertainty of the fatigue damage evaluations based on turbulence input. It also shows how the

annual fatigue reliability and sensitivity of reliability change in load channels of interest and different fatigue exponents.

760 ~~Furthermore, the reliability~~ The sensitivity analysis of the reliability reveals that although the change in the turbulence characterization changes the distribution of the fatigue loads and the fatigue reliability, it is more effective to focus on decreasing the material or models' uncertainty to have a more robust fatigue reliability assessment. This is because the overall importance of the fatigue loads compared to the high uncertainties in the material properties and linear damage accumulation rule is negligible in both load channels under study and different fatigue exponents. The change in the loads can vary. Furthermore, The reliability estimation is based on a simplified linearized limit state function, making which makes the complete separation of the loads from material properties possible. ~~If~~ In the case that all the random variables are lognormally distributed (which is highly possible), this formulation results in a very simple and fast reliability analysis at the design level.

770 ~~The importance ranks of the variables reveal that although the change in the turbulence characterization changes the distribution of the fatigue loads and the fatigue reliability, focusing on decreasing the material or models' uncertainty is more effective. This is due to the relatively high uncertainty in the material properties and linear damage accumulation rule.~~

Using Monte Carlo simulations, ~~considering other sources of uncertainty in the load, testing for other wind turbine designs and classes, using classes and the use of other aeroelastic tools, considering offshore cases, and finally, using different approaches for the design of experiments for the same study~~ are some suggestions for future studies.

Appendix Appendices

775 The parameters of the best-fitted distributions to $\log(DEL)$ in different load channels under study and different fatigue exponents are shown in Tables A1-D1.

Table A1. Best distribution fits to $\log(DEL_{lifetime})$ in different turbulence modeling cases considering flapwise bending moments in the blade root ($m = 8$)

| Case number | Distribution | Par 1 | Par-par 2 | Par-par 3 |
|---|---|-------|-----------|-----------|
| 1 (representative Representative turbulence) | lognormal (μ, σ) | 0.822 | 0.005 | - |
| 2 (lognormal turbulence) | lognormal (μ, σ) | 0.795 | 0.003 | - |
| 3 (Weibull turbulence) | lognormal (μ, σ) | 0.780 | 0.003 | - |

Figure ?? shows the distributions of $DEL_{lifetime}$ in two different cases of the study (Ed. 1 and Ed. 4) for the Siemens 2.3-MW. Different distributions of $DEL_{lifetime}$ considering 90% quantile of lognormal distribution and full distribution of Weibull for modeling the turbulence using the Siemens 2.3-MW as the case study

780 Table ?? shows the comparison of the probability of failure using FORM and MC in two scenarios (blade root $m = 10$ and tower base $m = 3$). Comparison of the probability of failure in years 10, 15, and 20 using Monte Carlo simulations and FORM for the blade ($m = 10$) and the tower ($m = 3$) **Component (fatigue exponent) Method P_f at year 10 P_f at year 15 P_f**

Table B1. Best distribution fits to $\text{Log}(DEL_{lifetime})$ in different turbulence modeling cases considering flapwise bending moments in the blade root ($m = 12$)

| Case number | Distribution | Par 1 | Par-par 2 | Par-par 3 |
|---|--|-------|-----------|-----------|
| 1 (representative <u>Representative</u> turbulence) | Normal (μ, σ) | 2.510 | 0.013 | - |
| 2 (lognormal turbulence) | Normal (μ, σ) | 2.457 | 0.007 | - |
| 3 (Weibull turbulence) | Normal (μ, σ) | 2.434 | 0.009 | - |

Table C1. Best distribution fits to $\text{Log}(DEL_{lifetime})$ in different turbulence modeling cases considering fore-aft bending moments in the tower base ($m = 4$)

| Case number | Distribution | Par 1 | Par-par 2 | Par-par 3 |
|---|---|--------|-----------|-----------|
| 1 (representative <u>Representative</u> turbulence) | lognormal (μ, σ) | 1.176 | 0.007 | - |
| 2 (lognormal turbulence) | GEV (μ, σ, ξ) | -0.218 | 0.012 | 3.044 |
| 3 (Weibull turbulence) | GEV (μ, σ, ξ) | -0.180 | 0.015 | 2.975 |

~~at year 20~~FORM 9.6×10^{-4} 1.1×10^{-2} 3.3×10^{-2} MC 8.9×10^{-4} 2.3×10^{-2} 1.1×10^{-1} FORM 4.2×10^{-7} 6.4×10^{-6}
 3.7×10^{-5} MC 3.9×10^{-7} 5.9×10^{-6} 3.4×10^{-5}

Table D1. Best distribution fits to $\text{Log}(DEL_{lifetime})$ in different turbulence modeling cases considering fore-aft bending moments in the tower base ($m = 5$)

| Case number | Distribution | Par 1 | Par-par 2 | Par-par 3 |
|---|--|--------|-----------|-----------|
| 1 (representative <u>Representative</u> turbulence) | GEV (μ, σ, ξ) | -0.169 | 0.023 | 3.396 |
| 2 (lognormal turbulence) | GEV (μ, σ, ξ) | -0.201 | 0.013 | 3.216 |
| 3 (Weibull turbulence) | GEV (μ, σ, ξ) | -0.194 | 0.017 | 3.162 |

785 *Author contributions.* SM, PV, and JR were responsible for the overall conceptualization of the study. SM wrote all the computer codes and performed all the data analysis. SM, PV, and KD were involved in the writing, and editing of the manuscript

Computational expenses of Monte Carlo in reliability assessment of wind turbine structural components

790 For low probabilities of failure, such as in structural components of the wind turbines, a lot of simulations are needed for MC. In a Monte Carlo analysis with N number of simulations, the coefficient of variation of the estimate ($P_f = 10^8$ in our case) is proportional to $1/\sqrt{N}$ (based on the law of large numbers). This means that if the actual probability of failure in a structural component is in the order of 10^{-x} , approximately $10^{(x+2)}$ simulations are needed to achieve an estimate with a coefficient of variance in the order of 10%. Standard computers can save data with size up to $N = 10^9$, meaning we can capture the maximum probability of failure 10^{-7} . It is possible to cluster the simulations, for example, to get 10 clusters of 10^9 to capture $P_f = 10^8$. However, more and more loops will take a lot of time for standard processors.

795 *Competing interests.* At least one of the (co-)authors is a member of the editorial board of Wind Energy Science.

Code and data availability

References

- Bacharoudis, K. C., Antoniou, A., and Lekou, D. J.: Measurement uncertainty of fatigue properties and its effect on the wind turbine blade reliability level, EWEA, November, pp. 17–20, 2015.
- 800 Bak, C., Zahle, F., Bitsche, R., Kim, T., Yde, A., Henriksen, L. C., and Natarajan, A., H. M. H.: Description of the DTU 10 MW Reference Wind Turbine, in: DTU Wind Energy Report-I-0092, July 2013.
- Basquin, O. H.: The Exponential Law of Endurance Tests, in: ASTM, p. 625, 1910.585
- Burton, T., Jenkins, N., Sharpe, D., and Bossanyi, E.: Wind energy handbook, John Wiley & Sons, <http://dx.doi.org/10.1002/9781119992714>, 2011.
- 805 Choi, S., Canfield, R. A., and Grandhi, R. V.: Reliability-Based Structural Design, Springer, <http://dx.doi.org/10.1007/978-1-84628-445-8>, 2007.
- ~~International Electrotechnical~~ Commission, G. I. E.: IEC 61400-1, Wind turbine generator systems – Part 1: Safety requirements, 3rd edition ed, Proceedings of the IEC, pp. 61 400–3, 2005.
- ~~International Electrotechnical~~ Commission, G. I. E.: IEC 61400-1, Wind turbine generator systems – Part 1: Safety requirements, 4th edition
810 ed, Proceedings of the IEC, 590 pp. 61 400–4, 2019.
- Dimitrov, N. K.: Structural reliability of wind turbine blades: Design methods and evaluation, Ph.D., Technical University of Denmark, 2013.
- Dimitrov, N. K., Natarajan, A., and Mann, J.: Effects of normal and extreme turbulence spectral parameters on wind turbine loads, Renewable Energy, 101, 1180–1193, <http://dx.doi.org/10.1016/j.renene.2016.10.001>, 2017.
- Dimitrov, N. K., Kelly, M. C., Vignaroli, A., and Berg, J.: From wind to loads: wind turbine site-specific load estimation with surrogate
815 models trained on high-fidelity load databases, Wind Energy Sci., 3, 767–790, <http://dx.doi.org/10.5194/wes-3-767-2018>, 2018.
- Emeis, S.: Current issues in wind energy meteorology, Meteorological Applications, 21, 803–819, 2014.
- Ernst, B. and Seume, J. R.: Investigation of site-specific wind field parameters and their effect on loads of offshore wind turbines, Energies, 5, 3835–3855, <http://dx.doi.org/10.1002/met.1472>, 2012.
- Gulvanessian, H. and Calgaro, J. and Holický, M.: Designer’s guide to EN 1990: eurocode: basis of structural design, Thomas Telford, 2002.
- 820 Hansen, K. S. and Larsen, G. C.: Characterising turbulence intensity for fatigue load analysis of wind turbines, Wind Engineering, 29, 600 319–329, <http://dx.doi.org/10.1260/030952405774857897>, 2005.
- Ishihara, T., Yamaguchi, A., and Sarwar, M. W.: A study of the normal turbulence model in IEC 61400-1, Wind Engineering, 36, 759–765, <http://dx.doi.org/10.1260/0309-524X.36.6.759>, 2012.
- ISO 2394, I.: General principles on reliability for structures, Zurich: ISO, 2015.
- 825 Kececioglu, D.: Reliability engineering handbook, vol. 1, DEStech Publications, Inc, 2002.
- Larsen, G. C.: Offshore fatigue design turbulence, Wind Energy An Int. J. for Progress and Applications in Wind Power Conversion Tech., 4, 107–120, <http://dx.doi.org/10.1002/we.49>, 2001.
- Larsen, T. J. and Hansen, A. M.: How 2 HAWC2, the user’s manual, target, 2, 2007.
- Le, X. and Peterson, M. L.: A method for fatigue-based reliability when the loading of a component is unknown, Int. J. of Fatigue, 21,
830 603–610, [http://dx.doi.org/10.1016/S0142-1123\(99\)00016-X](http://dx.doi.org/10.1016/S0142-1123(99)00016-X), 1999.
- Madsen, H. O., Krenk, S., and Lind, N. C.: Methods of structural safety, Courier Corporation, 2006.
- Mann, J.: Wind field simulation, Probabilistic Eng. Mech., 13, 269–282, [https://doi.org/https://doi.org/10.1016/S0266-8920\(97\)00036-2](https://doi.org/https://doi.org/10.1016/S0266-8920(97)00036-2), 1998.

- Márquez-Domínguez, S. and Sørensen, J. D.: Fatigue reliability and calibration of fatigue design factors for offshore wind turbines, *Energies*, 5, 1816–1834, <http://dx.doi.org/10.3390/en5061816>, 2012.
- Melchers, R. E. and Beck, A. T.: Structural reliability analysis and prediction, John Wiley & Sons, <http://dx.doi.org/10.1002/9781119266105>, 2018.
- Mikkelsen, L. P.: The fatigue damage evolution in the load-carrying composite laminates of wind turbine blades, in: *Fatigue Life Prediction of Composites and Composite Structures*, pp. 569–603, Elsevier, <http://dx.doi.org/10.1016/B978-0-08-102575-8.00016-4>, 2020.
- 835 Miner, M. A.: Cumulative damage in fatigue, <http://dx.doi.org/10.1115/1.4009458>, 1945.
- Mortensen, U. A., Rasmussen, S., Mikkelsen, L. P., Fraisse, A., and Andersen, T. L.: The impact of the fiber volume fraction on the fatigue on performance of glass fiber composites, *Composites-Part A: Applied Science and Manufacturing*, <http://dx.doi.org/10.1016/j.compositesa.2023.107493>, 2023.
- Mozafari, S., Dykes, K., Rinker, J. M., and Veers, P. S.: Effects of finite sampling on fatigue damage estimation of wind turbine components: A statistical study, *Wind Eng.*, <http://dx.doi.org/10.1177/0309524X231163825>, 2023.
- 845 Murcia, j. P., Réthoré, P., Dimitrov, N. K., Natarajan, A., Sørensen, J. D., Graf, P., and Kim, T.: Uncertainty propagation through an aeroelastic wind turbine model using polynomial surrogates, *Renewable Energy*, 119, 910–922, <https://doi.org/https://doi.org/10.1016/j.renene.2017.07.070>, 2018.
- Øistad, I. S.: Analysis of the Turbulence Intensity at Skipheia Measurement Station, Master's thesis, NTNU, 2015.
- 850 Palmgren, A.: Die lebensdauer von kugellagern, *Zeitschrift des Vereines Duetsher Ingenieure*, 68, 339, 1924.
- Rackwitz, R.: Aspects of structural reliability: in honor of R. Rackwitz, Herbert Utz Verlag, 2007.
- Rackwitz, R. and Fiessler, B.: Non-normal vectors in structural reliability, 1978.
- Ren, G., Liu, J., Wan, J., Li, F., Guo, Y., and Yu, D.: The analysis of turbulence intensity based on wind speed data in onshore wind farms, *Renewable energy*, 123, 756–766, <http://dx.doi.org/10.1016/j.renene.2018.02.080>, 2018.
- 855 Robertson, A. N., Shaler, K., Sethuraman, L., and Jonkman, J.: Sensitivity analysis of the effect of wind characteristics and turbine properties on wind turbine loads, *Wind Energy Sci.*, 4, 479–513, <http://dx.doi.org/10.5194/wes-4-479-2019>, 2019.
- Rognin, F., Abdi, F., Kunc, V., Lee, M., and Nikbin, K.: Probabilistic methods in predicting damage under multi-stage fatigue of composites using load block sequences, *Procedia Eng.*, 1, 55–58, <http://dx.doi.org/10.1016/j.proeng.2009.06.015>, 2009.
- Ronold, K. O., Wedel-Heinen, J., and Christensen, C. J.: Reliability-based fatigue design of wind-turbine rotor blades, *Eng. Struct.*, 21, 1101–1114, [http://dx.doi.org/10.1016/S0141-0296\(98\)00048-0](http://dx.doi.org/10.1016/S0141-0296(98)00048-0), 1999.
- 860 Schaff, J. R. and Davidson, B. D.: A strength-based wearout model for predicting the life of composite structures, ASTM special technical publication, 1285, 179–200, <http://dx.doi.org/10.1520/STP19928S>, 1997.
- Slot, R. M., Sørensen, J. D., Svenningsen, L., Moser, W., and Thøgersen, M. L.: Effective turbulence and its implications in wind turbine fatigue assessment, *Wind Energy*, 22, 1699–1715, <http://dx.doi.org/10.1002/we.2397>, 2019.
- 865 Srensen, J., D.: Reliability assessment of wind turbines, in: *Safety, Reliability, and Risk Analysis: Beyond the Horizon*, <http://dx.doi.org/10.1201/b15938-5>, 2015.
- Stensgaard, H. T., Svenningsen, L., Moser, W., Sørensen, J. D., and Thøgersen, M. L.: Wind climate parameters for wind turbine fatigue load assessment, *J. of Solar Energy Eng.*, 138, 031 010, <http://dx.doi.org/10.1115/1.4033111>, 2016a.
- Stensgaard, T. H., Svenningsen, L., Sørensen, J. D., Moser, W., and Thøgersen, M. L.: Uncertainty in wind climate parameters and their influence on wind turbine fatigue loads, *Renewable Energy*, 90, 352–361, <https://doi.org/10.1016/j.renene.2016.01.010>, 2016b.
- 870 Sndergaard, A. dL. and Jóhannsson, H. P.: Assessment of fatigue and extreme loading of wind turbines, M.S., Aalborg University, 2016.

- Toft, H. S. and Sørensen, J. D.: Reliability-based design of wind turbine blades, *Structural Safety*, 33, 333–342, <http://dx.doi.org/10.1016/j.strusafe.2011.05.003>, 2011.
- ~~Toft, H. S., Branner, K., Sørensen, J. D., Berring, P.: Reliability-based calibration of partial safety factors for wind turbine blades. EWEA, March 14–17, 2011.~~
- 875 Tsugawa, Y., Sakamoto, N., Kawasaki, S., Arakawa, C., and Iida, M.: Analysis of Wind Turbine Fatigue Loads for Proper Estimation of Offshore Turbulence Intensity, EWEA Offshore 2015, Copenhagen, 10–12 March 2015. POID:008.
- Türk, M. and Emeis, S.: The dependence of offshore turbulence intensity on wind speed, *J. of Wind Eng. and Ind. Aerodynamics*, 98, 466–471, <http://dx.doi.org/10.1016/j.jweia.2010.02.005>, 2010.
- 880 Veers, P. S.: Fatigue reliability of wind turbine components, 1990.
- Veers, P. S.: Statistical considerations in fatigue, *Journal of Fatigue and Fracture*, 19, 295–302, <http://dx.doi.org/10.31399/asm.hb.v19.a0002369>, 1996.
- [Velarde, J., Kramhøft, C., Mankar, A., and Sørensen, J. D.: Uncertainty modeling and fatigue reliability assessment of offshore wind turbine concrete structures. *Int. J. of Offshore and Polar Eng.*, 29, 165–171, <http://dx.doi.org/10.17736/ijope.2019.il54.2019>.](#)
- 885 Velarde, J., Mankar, A., Kramhøft, C., and Sørensen, J. D.: Probabilistic calibration of fatigue safety factors for offshore wind turbine concrete structures, *Eng. Struct.*, 222, 111 090, <http://dx.doi.org/10.1016/j.engstruct.2020.111090>, 2020.
- Veldkamp, D.: A probabilistic approach to wind turbine fatigue design, EWEC, Milan, Italy, 2007.
- Wang, H., Barthelmie, R. J., Pryor, S. C., and Kim, H. G.: A new turbulence model for offshore wind turbine standards, *Wind Energy*, 17, 1587–1604, <http://dx.doi.org/10.1002/we.1654>, 2014.
- 890 Yanan, C., Zhenand, S., and Shunhe, L.: Experimental study on fatigue behavior of composite laminate, *Acta Aeronautica et Astronautica Sinica*, 12, B643–B646, 1991.
- Zaccone, M.: Failure analysis of helical springs under compressor start/stop conditions, *Practical Failure Analysis*, 1, 51–62, <https://doi.org/10.1007/BF02715198>, 2001.